UCRL-17594

University of California

Ernest O. Lawrence Radiation Laboratory

THE EFFECT OF PERIODIC MENISCUS DISPLACEMENTS ON THE PERFORMANCE OF POROUS GAS ELECTRODES

Jean-Pierre Roussillon

August 1967

RECEIVED
LAWRENCE
RADIATION LABORAT
SEP 18 1967
LIBRARY AN
DOCUMENTS SEC

TWO-WEEK LOAN COPY

This is a Library Circulating Copy which may be borrowed for two weeks. For a personal retention copy, call Tech. Info. Division, Ext. 5545

UCRL-17594

DISCLAIMER

This document was prepared as an account of work sponsored by the United States Government. While this document is believed to contain correct information, neither the United States Government nor any agency thereof, nor the Regents of the University of California, nor any of their employees, makes any warranty, express or implied, or assumes any legal responsibility for the accuracy, completeness, or usefulness of any information, apparatus, product, or process disclosed, or represents that its use would not infringe privately owned rights. Reference herein to any specific commercial product, process, or service by its trade name, trademark, manufacturer, or otherwise, does not necessarily constitute or imply its endorsement, recommendation, or favoring by the United States Government or any agency thereof, or the Regents of the University of California. The views and opinions of authors expressed herein do not necessarily state or reflect those of the United States Government or any agency thereof or the Regents of the University of California.

UCRL-17594

UNIVERSITY OF CALIFORNIA
Lawrence Radiation Laboratory
Berkeley, California

AEC Contract No. W-7405-eng-48

THE EFFECT OF PERIODIC MENISCUS DISPLACEMENTS ON THE PERFORMANCE OF POROUS GAS ELECTRODES

Jean-Pierre Roussillon

(Masters Thesis)

August 1967

TABLE OF CONTENTS

I. INTRODUCTION 1

A. Development of the Film Theory of Porous Gas Electrodes... 2

B. The Film Model for Electrodes with a Single Pore Size..... 5

C. Transport Limitations and Possible Influence of Interface Movement 8

D. Previous Investigations Involving Perturbation of Gas-Electrolyte Interface 11

E. Scope of Present Work 13

II. DESIGN OF THE EXPERIMENT 14

A. Form of the Test Electrode 14

B. Choice of the Reaction System 15

C. Design of the Cell 17

D. Displacement of the Gas-Electrolyte Interface 18

E. Measurements of Electrode Operation 19

F. Experimental Conditions and Variables 20

III. EXPERIMENTAL EQUIPMENT 22

A. Cell and Electrodes 22

1. The Cathode 28

2. The Anode and the Reference Electrode 28

B. Mechanical Drive System 30

C. External Electrical Circuit 35

D. Systems for Filling the Cell with Electrolyte and for Gas Supply 38

TABLE OF CONTENTS (continued)

IV. EXPERIMENTAL PROCEDURE 41

A. Preparation of the Electrolyte 41

1. Titration of the Electrolyte 41

2. Degasification of the Solution 42

B. Filling of the Cell 43

1. Evacuation of the Cell-Reference Electrode System..... 43

2. Procedure for Filling the Cell 43

3. Gas Supply 45

C. Pre-Electrolysis 46

D. Conduct of the Measurements 47

1. Electrode Polarization Characteristics 48

2. Investigation of the Frequency and Amplitude of the Meniscus Movement 48

V. RESULTS AND DISCUSSION 50

A. Effects of the Meniscus Movement 50

B. Existence of an Electrolyte Short Circuit Path 63

C. Overpotential Measurements with Teflon Cathode Block 68

D. Summary 73

VI. CONCLUSIONS 75

ACKNOWLEDGEMENTS 76

REFERENCES 77

APPENDIX A: Reaction at the Counter Electrode 80

APPENDIX B: Estimation of Mass Transport Time Constants 82

APPENDIX C: Determination of the Current Range to be Investigated.. 84

APPENDIX D: Piston Displacement Amplitudes 86

APPENDIX E: Resistance of Electrolyte within the Capillary Tube Electrode 87

APPENDIX F: Oscillographic Recorder Traces for Experimental Runs... 88

THE EFFECT OF PERIODIC MENISCUS DISPLACEMENTS ON THE PERFORMANCE OF POROUS GAS ELECTRODES

Jean-Pierre Roussillon

Inorganic Materials Research Division, Lawrence Radiation Laboratory,
Department of Chemical Engineering, University of California
Berkeley, California

August 1967

ABSTRACT

The influence of periodic movement of the gas-electrolyte interface in a film type porous gas electrode was studied experimentally for the oxygen cathode in 2N potassium hydroxide electrolyte. A single silver capillary tube of 150μ inside diameter was used as a cathode. The interface motion was obtained by displacement of the electrolyte in a closed compartment by a small piston driven mechanically at controlled frequency and amplitude. Measurements of the response of the cathode potential relative to the mercury/mercuric oxide reference electrode were made under galvanostatic conditions. The results obtained could not be quantitatively interpreted because of the deviation of conditions in the capillary electrode from design conditions. These included the resistance of extraneous ionic current paths and variations in local electrode kinetic behavior along the pore wall. Nevertheless, qualitative effects of the méniscus movement were observed; they were characterized by a periodic response of the cathode potential of a few millivolts amplitude. These effects indicate a decrease in overpotential during the advance of the meniscus toward the gas filled portion of the capillary, and an increase during motion in the opposite direction, as might be expected on the basis of film electrode models.

I. INTRODUCTION

Porous gas electrodes have found a wide application in fuel cells and have been an important subject of research during this last decade. At present, although fuel cells are largely still in the research and the developmental stage, some of them can already produce power for long periods of time without attention. Most of the proposed reactants are gases, and hydrogen-oxygen fuel cells have already emerged for functional application in space programs.

Reactions of gaseous fuels and oxidants are usually conducted at porous gas electrodes which serve to separate the gas and the liquid electrolyte and which provide extended electrode surface areas. These electrodes consist of electrically conducting solid matrices interspersed with a system of connected pores. The pores are partially gas filled and partially flooded with electrolyte, the portion flooded being controlled through capillary action by the pore size distribution and the pressure differential across the electrode. The structure of the electrode is usually complex and may involve pores in more than one size range, as in the case of black platinum, carbon, and Raney alloy electrodes. For the case where the pores are all essentially the same size, electrodes can be effective only when the electrolyte wets the matrix and forms a film on the walls of the gas filled parts of the pore system, extending some distance beyond the electrode meniscus in the pore. The electrode reaction takes place primarily on the film covered pore walls. The behavior of such electrodes is strongly influenced by the diffusion of gas through the film of electrolyte, and by the transport of ionic species in the film, as well as by the kinetics of the electrochemical

reaction taking place at the electrode-electrolyte interface. Mass transport is thus a very important factor determining the performance of a gas electrode. Therefore, any phenomenon which would facilitate the gas and ionic species transport to or from the reaction sites should improve the electrode performance. The purpose of this investigation was to study the effects of periodic displacements of the gas electrolyte interface in a porous electrode with straight cylindrical pores upon the overpotential/current relationship of such an electrode.

A. Development of the Film Theory of Porous Gas Electrodes

As early as 1839, Grove[1,2] in his experiments involving a gas-electrolyte-electrode system discovered that a net increase of current occurs when part of a platinum sponge electrode is exposed to hydrogen gas above the level of the electrolyte. However, the importance of this experimental fact has been recognized only recently.

In 1957, Carl Wagner,[3] considering an oxygen cathode in molten salt electrolyte, proposed several models for the gas electrode. In one of them, he considered the existence of an adherent electrolyte film on the interior walls of gas filled portions of the pores of the electrode. He examined the different steps of the cathodic process: gas dissolution in the electrolyte, diffusion to the electrode surface, and reduction at the surface. Making several simplifying assumptions, Wagner developed mathematical analysis of his models and compared their predictions.

A surface diffusion mechanism also discussed by Wagner had already been proposed by Justi et al.[4] in 1956. In the surface diffusion theory, the electrolyte forms a sharp circular three-phase boundary along the pore wall. Atoms of gas are adsorbed on the dry electrode surface and

diffuse along the walls to the electrolyte filled part of the pore where they react. The equations derived for this theory were later claimed to be applicable to the film model by Justi.[5]

In 1963, Will[6,7] studied the electrochemical reaction of hydrogen at the exterior of cylindrical platinum electrodes in sulfuric acid solutions. For a given potential, he measured the current as a function of the electrode position. The reaction was found to take place almost exclusively in a narrow region above the upper edge of the intrinsic meniscus. Gas diffusion through a film appeared to be the controlling step, and Will explained the limitations of the reaction region by a large ohmic voltage drop along the film paralleled with the electrode surface, associated with the migration of hydrogen ions. He also found that the diffusion of hydrogen molecules through the bulk of the electrolyte below the top of the meniscus represents only a very small contribution to the overall current. Will developed a model for the film theory assuming an equilibrium reaction and a film of uniform composition.

Using data obtained for the oxidation of hydrogen on a nickel electrode with sodium hydroxide electrolyte, Iczkowski[8] later developed a numerical solution for a film model of a gas electrode at high and low currents. He also solved numerically Justi's equations. Comparing the results obtained for the surface diffusion mechanism and for the film electrolyte mechanism, he concluded that the film theory offers the most likely explanation for the observed behavior of the electrode. With the assumption that hydrogen diffusion is the rate limiting factor, the theoretically calculated currents are in agreement with the experimental studies done by Will. For a pore of 5μ, it was found that the reaction takes place essentially within 0.002 cm above the meniscus.

Both Will and Iczkowski limited their study to the cases where gas diffusion through the electrolyte film is the only rate-determining process. However, since the limiting diffusion currents may have a greater order of magnitude than the exchange current densities for many gas reactions, Grens et al.[9] developed a model in which the effects of kinetic limitations for the reaction, as well as variations in electrolyte composition in the film, were also considered. It was found that, under many circumstances, the reaction occurs over a length equal to thousands of film thicknesses above the meniscus and that diffusion of dissolved gas is often not the controlling process. Such conclusions could be expected to hold for the oxygen cathode and other gas reactions with low to moderate exchange current densities. This last model is in agreement with the experimental results obtained by Katan et al.[10] for an oxygen cathode formed of a bed of very small silver spheres and operated in concentrated potassium hydroxide solutions.

Starting with a model similar to the one used above which involves a single pore whose gas filled part is coated by a thin film of electrolyte, Rockett[11] independently developed an analysis incorporating electrode kinetic limitations and variations in electrolyte composition. He found that the region where the reaction takes place is polarization dependent and that water is transported in the gas phase. From his experimental results, Rockett concluded that the performance of a gas electrode would not be limited by one effect but by an interplay of several.

In 1964, Bennion[12] measured the current density distribution for an oxygen cathode consisting of the exterior surfaces of nickel and

silver cylinders partially immersed in potassium hydroxide solutions. His experimental results showed that the reaction zone extends well above the apparent meniscus under the electrolyte film. His theoretical analysis based upon the measurements indicated that the current density distribution is controlled by a balance between kinetic overpotential and ohmic voltage drop in the film. The results also suggest a water transport effect in the gas phase.

An experimental demonstration of the presence of a film of electrolyte and a determination of its thickness were given by Pshenichnikov,[13] who investigated the process taking place on smooth nickel hydrogen electrodes partially immersed in potassium hydroxide solution. Assuming that the diffusion of hydrogen molecules through the film is not the slow step, Pshenichnikov obtained a good coincidence between his theoretical and experimental results.

The existence of a thin electrolyte film above the meniscus was also observed experimentally by Muller[14,15] who used interferometric techniques during the reduction of oxygen on nickel and silver surfaces partially immersed in potassium hydroxide solutions.

B. <u>The Film Model for Electrodes with a Single Pore Size</u>

The developments cited above lead to the film model for porous gas electrodes whose pores are all of much the same size. Other models are required to represent electrodes with wide pore size distributions or with pores rendered partially lyophobic. In its simplest form, this model reduces to a single pore of uniform section partly filled with electrolyte. In most studies, the interface has been considered to be a plane surface. The wall of the gas filled portion of the pore is

covered by a thin film of electrolyte extending far beyond the intrinsic meniscus. The thickness of this film is of the order of 0.01 - 1μ and is usually assumed to be constant. One possible mechanism of formation of such stable supermeniscus films was given recently by Lightfoot,[16] who tried to explain their existence.

As represented in Fig. 1, a pore can be divided into three regions for which different effects must be considered. In the first region, where the gas filled portion of the pore is well removed from the meniscus, the gas phase transport is the principal phenomenon occurring; the role of this region is more important in the case of a gas mixture than of a pure reactant. The second region consists of the reaction zone, extending from slightly in the liquid side of the meniscus to a distance perhaps equal to thousands of film thicknesses into the gas filled part of the pore. Here the gas dissolves in the electrolyte and diffuses across the film to the electrode surface where the electrochemical reaction takes place. The ionic species produced or consumed by the reaction move along the film to the flooded part of the pore by diffusion and migration. The local reaction rate is governed by the kinetic relationship involving local electrode potential and dissolved gas and ionic species concentrations. The electrons involved in the process are carried by the electrode matrix. Finally, in the electrolyte flooded part of the pore, there is transport of ionic species moving axially, driven by concentration and potential gradients.

For most electrodes, the processes determining the overpotential/current density relationship for the electrode are those in the second, or reaction, zone. Thus, it is here we must augment the transport phenomena if we are to affect the electrode performance.

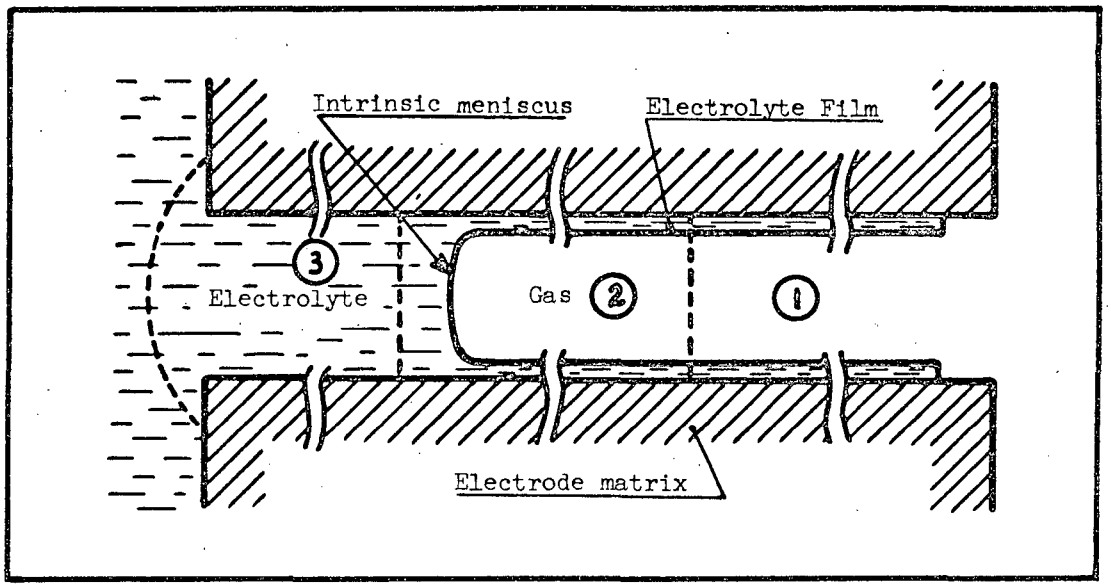

XBL 676-4115

Fig. 1 Representation of film type gas electrode.

C. Transport Limitations and Possible Influence of Interface Movement

As can be seen from the film model just described, mass transfer, which is characterized by migration and diffusion of ionic species along the electrolyte film and by gas diffusion across the electrolyte film, is certainly one of the important factors in the determination of the performance of gas electrodes. One main factor limiting the electrochemical reaction taking place under the electrolyte film is the transport of ionic species along the film. The potential drop associated with this transport reduces the overpotential, and thus the reaction rate, at sites well removed from the meniscus. The concentration gradient established in absence of convection also creates concentration overpotential opposing the reaction. This is the case for the reaction zone BC represented in Fig. 2a. In this figure, the gas (G) dissolves at the electrolyte surface and diffuses through the electrolyte to reaction sites at the pore wall, both under the film and in the flooded part of the pore just below the meniscus. The dissolved gas reacts at the electrode surface, forming or consuming ionic species (S). Beyond point C, the potential in the film is too low for the reaction to take place at a significant rate. In the electrolyte filled part, zone AB, transport of ionic species is much easier, and the potential is almost uniform. However, here the reaction is limited by diffusion of gas to the electrode surface, which now must occur over a distance many times greater than the thickness of the film. Thus, one possible approach to improvement of the performance of this film type gas electrode is to increase transport of either ionic species in the electrolyte film or the dissolved gas below the meniscus.

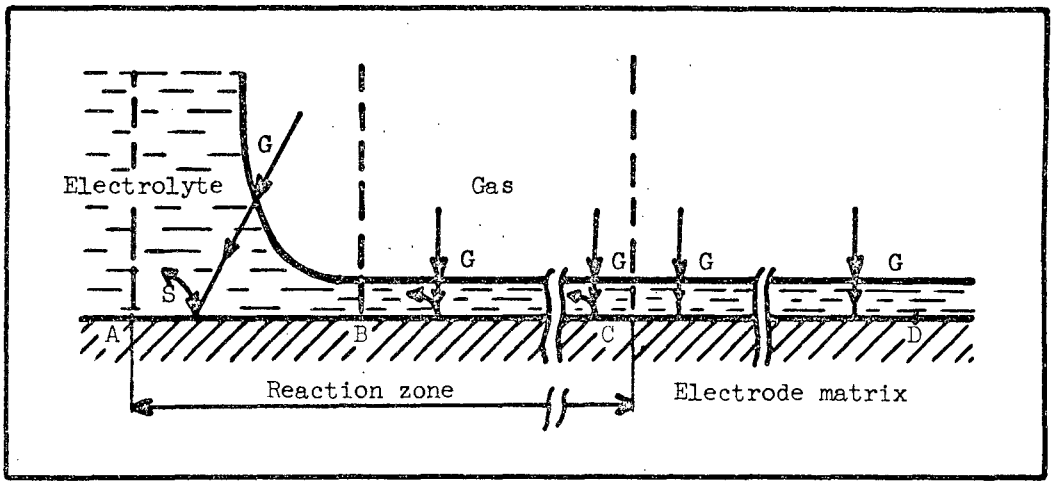

Fig. 2a

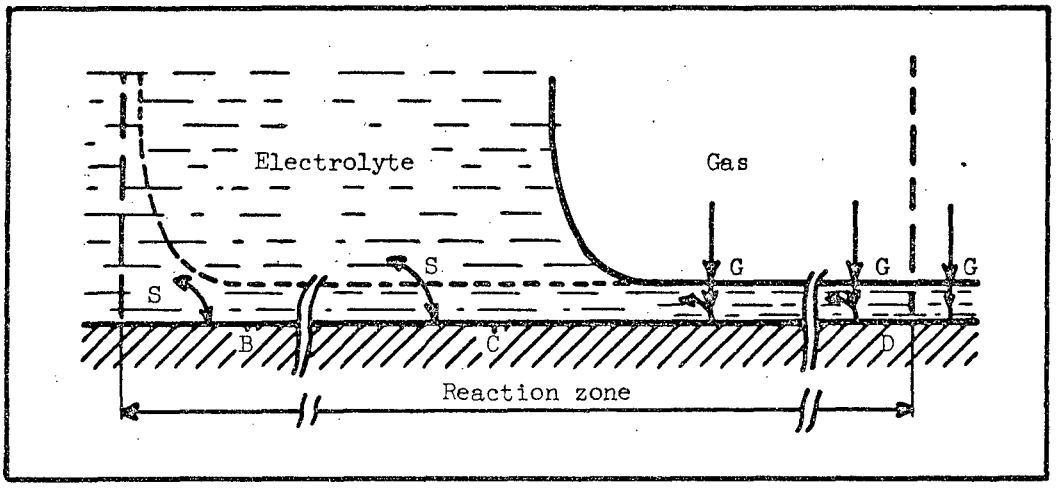

Fig. 2b

XBL 676-4116

Figs. 2 Representation of effect of meniscus displacement of film electrode model.

It might appear to be advantageous to create or increase convection in the film. However, the existence of convection that results in mixing in the electrolyte film has different effects for reactions in which ions are consumed and for those in which ions are produced. In the first case, the convection serves to overcome the depletion of ions in the film at positions distant from the meniscus and thus facilitates transport of current in the film; this effect, together with elimination of concentration overpotential, results in an improvement in electrode performance (higher currents at a given overpotential). In the second case, the convection eliminates the accumulation of ions in the film and thus adversely affects current transport; here this effect is partly balanced by elimination of the concentration overpotential. A theoretical analysis derived by Lightfoot[17] confirms that any increase of convection in the film should not improve the performance of a film type porous gas electrode in which ions are produced during the reaction. Another possible effect of convection in the film is improved dissolved gas transport through the film. However, for the very thin films encountered in gas electrodes this effect cannot be very large.

Another possibility for improvement of the performance of a film type gas electrode is to increase the gas concentration at the electrolyte-electrode interface in the flooded part of the pore. One way of accomplishing this is to move the meniscus toward the gas filled part of the pore, as shown in Fig. 2b. This brings dissolved gas at the electrode surface to the flooded part of the pore where the potential is more favorable for the reaction. Before the gas-electrolyte interface displacement, the surface represented

between the points C and D was covered with electrolyte in equilibrium with the gas partial pressure while the concentration between B and C where the reaction was taking place was somewhat lower. (During the displacement of the meniscus, it may be assumed that the part of the electrolyte film nearest the wall is essentially stationary because of the drag of the wall of the pore.) Therefore, after displacement of the interface, the gas concentration at the electrode surface below the meniscus should be sufficient for the reaction to take place in this part of the pore where transport of ionic species is easy. Moreover, the reaction zone above the meniscus will still extend over the same length, and more favorable dissolved gas concentration now also exists here as a result of the displacement. This situation only exists so long as movement of the meniscus continues. Once it stops, the dissolved gas in the flooded part of the pore is soon used up. The effect to be expected during a displacement of the meniscus toward the electrolyte filled part of the pore is not entirely clear but can be expected to be in an opposite direction. It is difficult to predict the global effect of a periodic movement of the gas-electrolyte interface for a film type porous gas electrode, but it is possible that the average overpotential of the electrode will be affected. An investigation of the influence of such movement appears to be justified.

D. Previous Investigations Involving Perturbation of Gas-Electrolyte Interface

The only reported study of moving the gas-electrolyte interface was by Kordesch and Kronenberg[18] who thought that, besides having an influence on mass transfer, the perturbation of the interface could also

decrease the activation overpotential in the case of a poor catalyst or reduce the deterioration of catalyst activity with usage. Such phenomenon may effectively exist with a catalyst surface that can be reactivated during the interface displacement as in the example, given by Kronenberg, of an oxide operating in a reducing atmosphere.

The experimental study of the possible effect of the gas-electrolyte interface modification was carried out by Kordesch in 1963. Working with hydrophobic and hydrophilic electrodes, he disturbed the interface by electrolyte pressure pulses over a wide range of frequencies. Experiments involving such mechanical pulsing of the electrolyte were conducted on carbon, metal, and thin composite electrodes in the range of 0 to 450 cycles/minute. Different gases including hydrogen, oxygen, and air were used with potassium hydroxide electrolyte. Pressure pulses of 9 to 24 psia were applied to the electrolyte and caused modification of the interface throughout the electrodes, which were 0.045 inch and 0.25 inch thick. Taking polarization curves before, during, and after pulsing, Kordesch never observed a change of the cell voltage greater than a few millivolts and concluded that the main effect was an accelerated "breaking in" phenomenon. In general, it was found that the most significant change in the electrode performance was taking place between the prepulsing and the first pulsing run, no special effect being noted at any particular pulsing frequency. Other experiments completed at sonic frequencies also showed no significant effect on the cell performance.

Experiments involving the mechanical vibration of the electrode were investigated but did not reveal any significant results. Four different modes of electrical disturbance, namely interrupted direct current,

alternating current superimposed on direct current, charge-discharge cycling, and heavy discharge pulsing were also studied. Significant effects were mentioned only with heavy discharge pulsing, but results were not completely reported.

Most of the experiments done by Kordesch were conducted on carbon and thin composite electrodes, and did not permit him to control the movement of the gas-electrolyte interface. Therefore, no relation between the different parameters could be derived from his results.

E. Scope of Present Work

The purpose of this investigation is to determine the effect of the frequency and amplitude of the periodic displacement of the gas-electrolyte interface in a film type porous gas electrode. The experiments were conducted on an oxygen cathode with potassium hydroxide electrolyte. The electrode used was a single silver capillary tube of .15 mm inside diameter. Sinusoidal displacement of the meniscus with controlled frequency and amplitude was obtained by use of a micropiston moving in the electrolyte compartment of the experimental cell. Measurements of the response of the electrode potential were made under galvanostatic conditions over a range of currents. Unfortunately, severe deviations from design conditions were encountered during the experiments, which have precluded any quantitative interpretation of the data.

II. DESIGN OF THE EXPERIMENT

In order to study experimentally the effects of the displacement of the gas-electrolyte interface in a film type porous gas-electrode, certain requirements must be met. First, the electrode reaction must be well behaved and well enough described to permit analysis of the effects. Second, the meniscus position must be subjected to a movement that can be easily characterized and controlled. Finally, the electrode performance and the meniscus position must be continually measured during the displacement. The manner in which these requirements are to be satisfied is discussed in the following section.

A. Form of the Test Electrode

The structure of a porous gas electrode is so complex that the matrix, a conducting solid with an arrangement of tortuous pores, cannot be well described, and the movement of the gas-liquid interface within it cannot be characterized. As previously stated, models for a film type electrode often assume a regular distribution of parallel, straight, cylindrical pores of equal diameter. Each of these pores is partly filled with electrolyte and each contributes the same increment to the total electrode current. Therefore, to use a cathode made by the assembly of parallel capillary tubes is an attractive idea. However, because of inevitable variations in diameter and wall surface for real capillaries of small diameter, it would be impossible to provide identical, or even similar, meniscus movements in a collection of such tubes in any conceivable manner. Consequently, it was decided to use a single capillary tube electrode, in spite of the limitation this places on the current levels used in the investigation. The

diameter of this tube should be as small as possible to provide a model close to a real pore of perhaps .1 - 5μ. However, it is difficult to obtain metal capillary tubes with an inside diameter smaller than 100 - 150μ. Also, the use of a smaller tube would create a problem for the motion of the gas-electrolyte interface. Therefore, a capillary tube of the smallest size available (150μ specified inside diameter) was chosen. This tube must be long enough to permit displacements of the meniscus but also small enough to permit its mounting in the cell. An electrode of 2 cm length was chosen.

B. Choice of the Reaction System

It is of special interest to study the effect of the perturbation of the gas-electrolyte interface on the performance of gas electrodes of practical importance. Moreover, the electrochemical behavior of the system used in this investigation must be well understood to allow analysis of the experimental results. This led to the restriction of the choice of reactants to oxygen and hydrogen.

The reaction zone, described in the previous chapter, extends further above the gas-electrolyte interface for smaller exchange current densities, as shown by Grens et al.[9] The effect of the displacement of the gas-electrolyte interface might be expected to be of more significance for an electrode with a relatively large reaction zone. Therefore, the oxygen electrode was preferred to the hydrogen electrode which has a much higher exchange current density.*

---

* The exchange current density for an oxygen electrode on a silver cathode with a 6.8N solution of potassium hydroxide has been given as 2×10^{-6} A/cm^2,[10] while the exchange current density for an hydrogen electrode on smooth platinum is reported to be 10^{-4}A/cm^2 for a 2N solution of sulfuric acid, or 10^{-3} A/cm for a 1N solution of hydrochloric acid.[19]

Mixing flows in the electrolyte film reduces the concentration gradients built up in absence of convection. In the case of an electrochemical reaction in which ionic species are consumed, the effect of convection is to improve the performance of the electrode, as discussed in the previous chapter. Therefore, experimental results obtained for a reaction that consumes ionic species would be difficult to interpret since the performance of the electrode might be affected by an increase of convection in the film as well as by the movement of the gas-electrolyte interface. Consequently, it was necessary that this investigation be concerned with a reaction producing ionic species. Since oxygen was chosen as the gaseous reactant, a strong base was necessarily used as the electrolyte. Many experimental works realized with an oxygen electrode were conducted with potassium hydroxide electrolyte. Solutions of potassium hydroxide have a high surface tension which allows a thin isothermal film with only a very small concentration gradient, as shown by Lightfoot.[16] Moreover, the solubility and diffusion coefficients of oxygen in potassium hydroxide solutions are well known.[20] Therefore, a solution of potassium hydroxide has been chosen as electrolyte. Thus, the reaction considered is:

$$O_2 + 2H_2O + 4e \rightleftharpoons 4OH^-$$

This reaction is important in low temperature fuel cells. It also presents the advantage of taking place on certain metal surfaces without use of special catalysts. One metal which satisfies this property is silver. Also, data are available for oxygen reduction on silver in potassium hydroxide solution, such as the kinetic data of Katan,[21] and those recently obtained by Beer[22] for current/voltage

characteristics. Since it was possible to purchase silver capillary tubes, these experiments were conducted with the system oxygen/silver/potassium hydroxide.

C. Design of the Cell

A gas-electrolyte interface inside the capillary tube can be obtained only if one end of the capillary is immersed in the electrolyte while the other side gives free access to the reactant gas. Therefore, the cathode was set in a support which separates the inside of the cell into two compartments, one for the potassium hydroxide solution and the other one for oxygen. To study the cathode under conditions of imposed current, a counter-electrode had to be provided to complete the cell circuit. Since the electrolyte was a solution of potassium hydroxide, the counter-electrode must not react spontaneously with a strong base. Moreover, the reaction taking place at the counter-electrode must not involve ionic species not already present in the electrolyte. This requirement led to use of a metal/metal oxide electrode; nickel was chosen. Then, the overall reaction can be written:

$$Ni + 2OH^- \rightarrow Ni(OH)_2 + 2e$$

However, in alkaline solution, the following reaction that would evolve oxygen bubbles may also be expected:

$$4OH^- \rightarrow O_2 + 2\,H_2O + 4e$$

By considering the equilibrium potentials of both reactions, it is shown in Appendix A that the first reaction is most likely the only one taking place in such conditions. Since $Ni(OH)_2$ is practically

insoluble in potassium hydroxide,[23] the concentration of nickel ions in the electrolyte should stay very small during the experiments.

The cathode voltage is measured relative to a reference electrode, which must be highly reproducible and compatible with the electrolyte. A mercury/mercuric oxide reference electrode satisfies these requirements. Also, its equilibrium potential is independent of the form of the mercuric oxide used and of the concentration of the solution of potassium hydroxide.[24]

D. Displacement of the Gas-Electrolyte Interface

Both frequency and amplitude of the movement of the gas-electrolyte interface should be known. For this reason a positive displacement of electrolyte is necessary, rather than pressure perturbations, which would not permit any control of the meniscus movement amplitude. If the solution is assumed to be incompressible, the change of volume of electrolyte inside the capillary tube necessary for the displacement of the meniscus requires an equivalent change in volume of the electrolyte compartment. One method of achieving this is by use of a small piston moving into a fixed volume of electrolyte.

The movement of the gas-electrolyte interface that would be the simplest to analyze is the case of constant velocity. However, it is not possible to keep moving the meniscus in one direction inside a tube of finite length. Therefore, the meniscus must be displaced in both directions, and a periodic movement will be studied. Since it is difficult to obtain a displacement of the meniscus with sudden changes in velocity, a sine movement, which does not involve any high derivatives and is convenient for theoretical analysis and generation, was chosen. A range of amplitudes and frequencies of the meniscus move-

ment should be available to permit a comprehensive study of the phenomenon. Since the change of volume of the electrolyte compartment required to move the gas-electrolyte interface in the capillary tube is very small, the piston diameter should be as small as possible. However, the smallest piston that could be obtained was .152mm diameter, which is the same size as the inside diameter of the cathode. Consequently, the amplitude of the piston movement must be equal to the amplitude of the meniscus displacement in the electrode. This requires a flexible drive system for the piston mechanism. Moreover, the effect of the meniscus movement can be studied only if the different frequencies investigated are constant. This requirement implied a controlled speed drive system.

E. Measurements of Electrode Operation

The effects of meniscus perturbations are of interest under both galvanostatic and potentiostatic conditions. The availability of supporting electronic equipment has dictated the galvanostatic method for these experiments. Under these conditions, the electrode overpotential was the important performance characteristic. Consequently, the cathode voltage relative to the reference electrode was studied as a function of the gas-electrolyte interface movement for a constant current provided by a power supply driving the cell. In any evaluation of such results, consideration should be given to variations of voltage drop which are due to the change of resistance of the electrolyte filled part of the capillary tube during the displacement of the meniscus. In fact, as the gas-electrolyte interface is moved toward the gas end of the capillary tube, the electrode overpotential may be expected to decrease while the ohmic drop increases, and when the meniscus is moved

toward the electrolyte side of the tube the overpotential may increase while the ohmic drop decreases. This effect will always be in phase with the movement of the gas-electrolyte interface but its exact magnitude will depend on the reaction distribution in the vicinity of the meniscus.

Since it is necessary to measure currents without interference of any other currents involved in spurious reactions at metal parts in contact with the electrolyte, the piston should be maintained at the counter electrode potential. This dictates grounding the counter electrode, as well as the piston, and operating the cathode at a potential negative with respect to ground.

The cathode response to the periodic displacement of the gas-electrolyte interface can be quantitatively investigated only if the piston movement is known. Moreover, the study of phase lags, which may be interesting, requires a determination of the meniscus movement. Therefore, in order to relate the electrical response to the meniscus displacement, both the cathode potential relative to the reference electrode and the piston movement must be continuously recorded.

F. Experimental Conditions and Variables

Although the temperature and concentration of the electrolyte determine the cathode potential, the influence of these two parameters is not an object of this investigation. Accordingly, all experiments were conducted at room temperature in order to simplify temperature control. The solubility and diffusion coefficient of oxygen in a solution of potassium hydroxide decrease with increasing concentration, while the conductivity increases with increasing concentration. Consequently, a moderately concentrated solution is indicated and a 2N potassium hydroxide solution was selected.

The smallest gas-electrolyte interface displacement of interest is of the order of the pore diameter. Moreover, it is practically difficult to move the meniscus with an amplitude less than .1mm. As for the upper limit of the displacement amplitude, it simply has to be small compared to the total length of the electrode. Interesting effects should be encountered for amplitudes of the meniscus movement equal to at least the length of the reaction zone. Therefore, measurements were made for amplitudes ranging from .1mm to 2.6 mm.

The range of frequencies to be investigated is determined by mechanical limitations and by the response of the electrode potential. As a first approximation, the mass transport time constant for the electrode may be of the order of a small fraction of a second up to a few seconds, as shown in Appendix B. This indicates a frequency range of interest of about .05 - 1000 Hz. The lowest frequency that can be reached with a convenient mechanical drive system is approximately .1 cycles/sec, and the highest about perhaps 20 cycles/sec. This investigation, at least initially, must be confined to this range.

The influence of the frequency and amplitude of the gas-electrolyte interface movement should be experimentally studied for different electrode currents. Assuming that the results obtained by Grens[9] hold for this particular electrode, currents of interest for a capillary tube electrode of .150mm diameter range from approximately 5×10^{-8}A up to 5×10^{-6} A, as shown in Appendix C. Initial experiments were run with currents of this magnitude.

III. EXPERIMENTAL EQUIPMENT

The equipment used in this investigation was constructed according to the concepts developed in the previous chapter. It can be divided, according to function, into four components: the cell, the mechanical drive system, the electrical circuit, and the auxiliary system used for filling the cell with electrolyte and used for gas supply. The cell and associated equipment are shown in Fig. 3.

A. Cell and Electrodes

The cell used for these experiments is shown in Figs. 4 and 5. It consists of two compartments, one for the reactant gas and one for the electrolyte, joined by the capillary tube cathode. The gas compartment has approximately the shape of a cylinder of 26 mm diameter and 50 mm length. On the other side, the electrolyte compartment is in the shape of two cylinders of different diameters stacked with the same axis; their dimensions are respectively 50 mm diameter by 15 mm length and 15 mm diameter by 25 mm length. The body of the cell is about 96 × 96 × 90 mm. It has approximately the shape of a cube with two cylindrical ends of 15 mm thickness whose diameter is about equal to the cube diagonal. A drawing of the central part of the cell with the main dimensions is represented in Fig. 6. Two flat circular end plates of 11 mm thickness and 120 mm diameter close the gas and electrolyte compartments. The cell is made of lucite because this material is transparent, easy to machine, and has fair thermal insulating properties. The external surfaces of the main body are polished to permit observations of the electrodes.

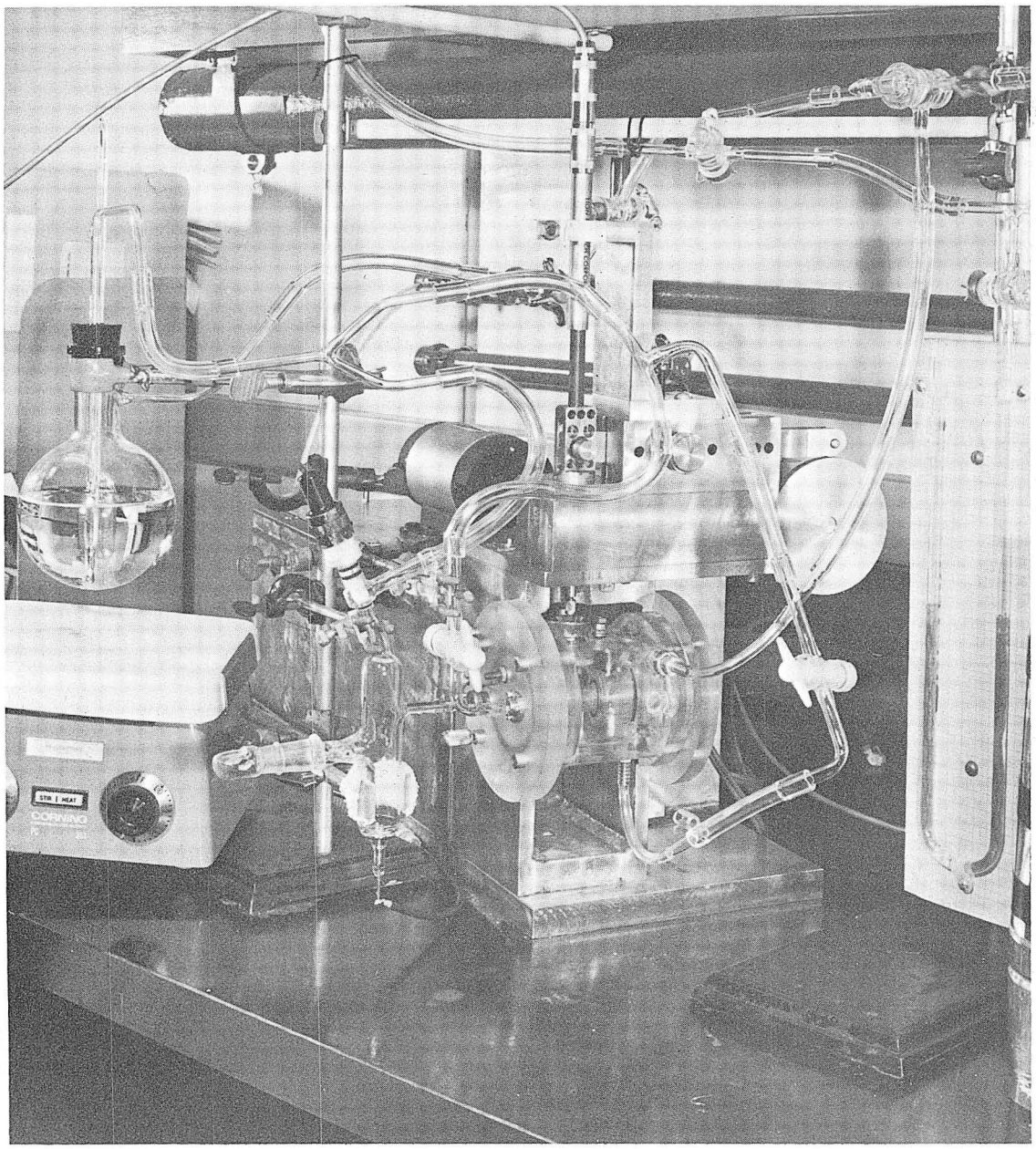

XBB 675-2733

Fig. 3 General view of experimental equipment.

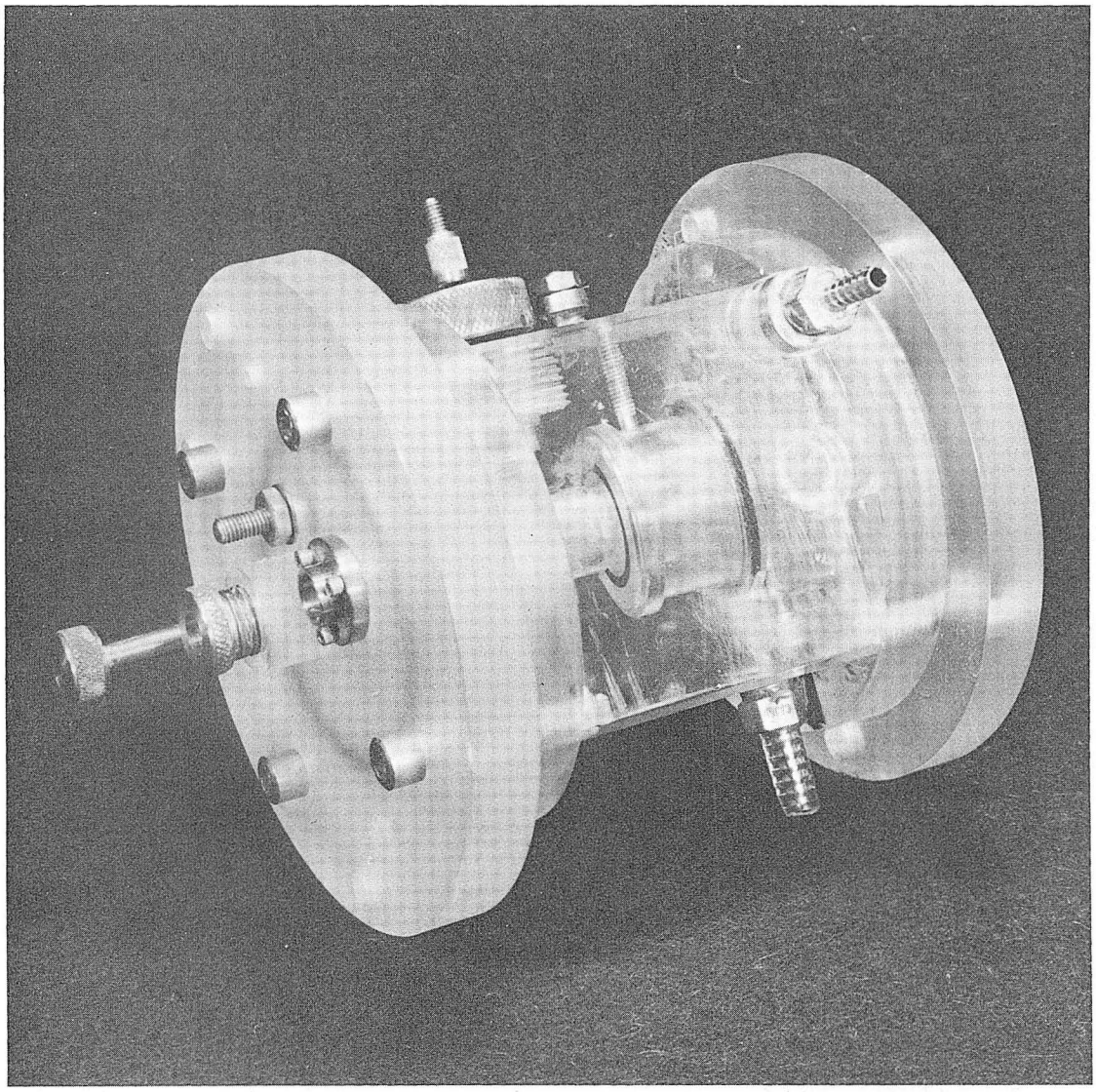

XBB 675-2735

Fig. 4 Cell (gas side to right).

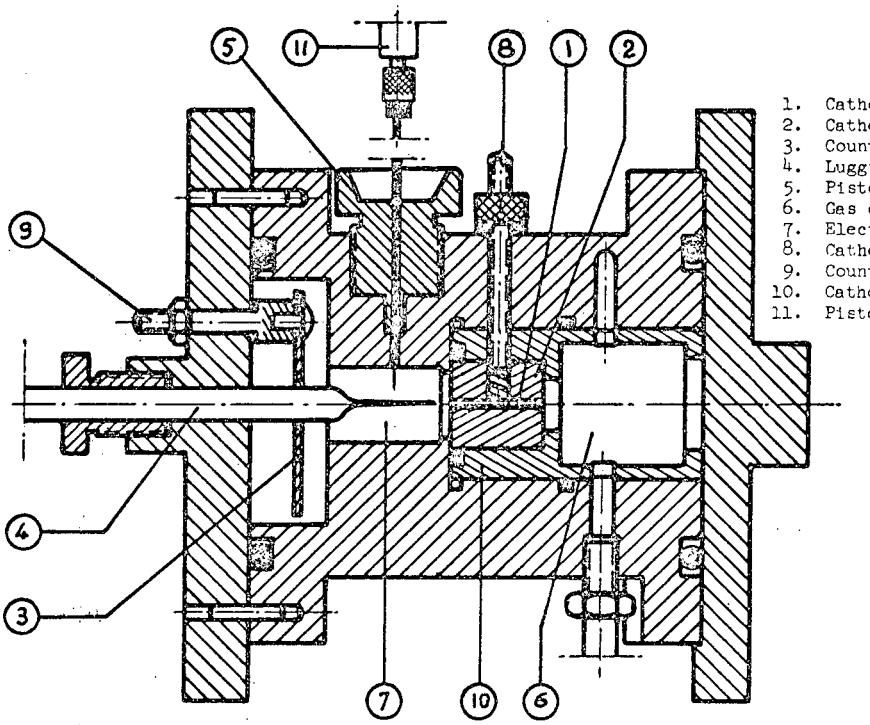

1. Cathode
2. Cathode block
3. Counter electrode
4. Luggin capillary
5. Piston assembly
6. Gas compartment
7. Electrolyte compartment
8. Cathode terminal
9. Counter electrode terminal
10. Cathode support
11. Piston carrier

XBL 676-4117

Fig. 5 Vertical section along cell axis.

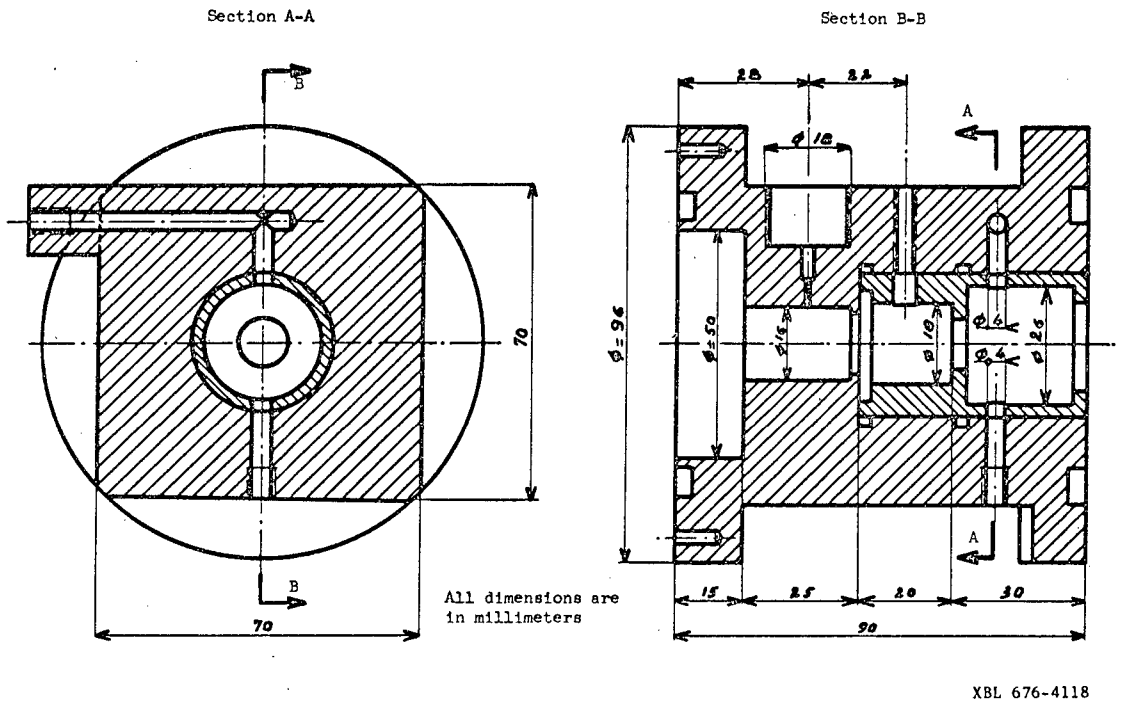

XBL 676-4118

Fig. 6 Cell sections.

Certain cell accessories are also shown in Fig. 5. The piston assembly for electrolyte displacement is screwed into the top wall of the electrolyte compartment. The cathode terminal (8) is also screwed into the top wall of the main block while the counter electrode terminal (9) is on the electrolyte compartment end plate. The two other accesses through this end plate, which can be seen in Fig. 4, are for the Luggin capillary (4) and a glass valve used for filling the cell. A device used for the adjustment of the gas-electrolyte interface position in the capillary is also mounted in this end plate. It consists of a screw, whose pitch is 40 threads per inch, ended by a small cylindrical piston of 3.175 mm diameter. Movement of this piston into or out of the electrolyte compartment changes the volume of the compartment and thus displaces the mean location of the meniscus in the capillary tube. O-ring seals are used at the circle of contact of the two end plates with the cell and around the piston assembly, the Luggin capillary tube, the meniscus positioning device, the cathode and counter electrode terminals, and the hose connections shown in Fig. 4. All metal parts in contact with the electrolyte, except the electrode and the piston, are type 304 stainless steel.

The thermal capacity of the cell is large enough to inhibit any significant temperature changes and therefore, no additional thermal insulation is required. However, the reference cell has turned out to be very sensitive to short term temperature variations and, consequently, is insulated with an approximately 5 cm thick layer of Fiberfrax ceramic fiber insulation.

1. The Cathode

The oxygen cathode consists of a thick-walled silver capillary tube of .15 mm inside diameter, 1.27 mm outside diameter, and 20 mm length*. This tube is cemented in a cylindrical lucite block (2) of 12 mm diameter which is assembled in the cell by the cathode support (10), as shown in Fig. 5. Two O-rings are installed to avoid leakage around either the cathode support or the cathode block. The cathode support is held in position by the end plate of the gas compartment. Electrical contact to the cathode is made by a screw (8) passing through a small spring so as to avoid damage to the capillary tube.

2. The Anode and the Reference Electrode

The anode, or counter-electrode, is a simple disk of porous nickel of 50 mm diameter and 2 mm thickness. A hole in its center is provided for the passage of the Luggin capillary of the reference electrode, as shown in Fig. 5. The counter electrode is supported by a stainless steel rod that fits through the electrolyte compartment end plate. The other end of the rod provides the electrical contact to the anode. Leakage where the rod passes through the end plate is prevented by an O-ring seal.

The reference electrode, shown in Fig. 7, is mounted outside the end plate on the electrolyte side of the cell. It is a vertical glass cylinder of 25 mm diameter and 110 mm height, with a platinum contact

* Purchased from: The Wilkinson Co., 1660 -9th St., Santa Monica, Calif.

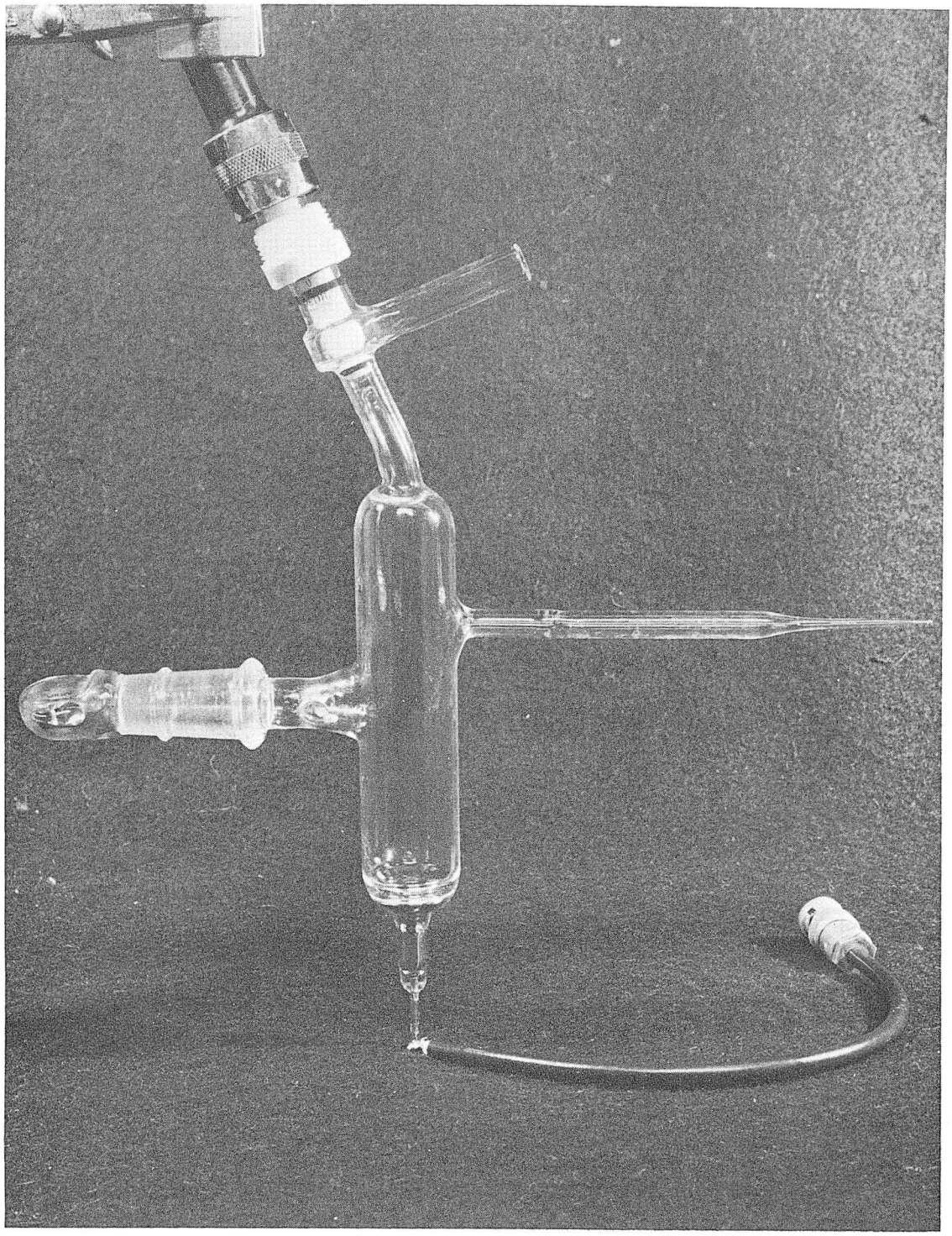

XBB 675-2734

Fig. 7 Reference electrode cell.

wire in the sealed lower end connected through a tungsten-uranium glass seal to an external electrical terminal. The platinum wire is submerged in a pool of mercury 1.5 cm deep, which is in turn covered by a thin layer of mercuric oxide*. An opening, closed by a 12 mm standard taper glass joint, is provided about half-way up the side of the reference cell for introduction of mercuric oxide. A Delmar needle valve stopcock of 9 mm diameter is fitted at the upper part of the reference cell to permit the evacuation of the cell and its filling with electrolyte. A Luggin capillary leads from the reference electrode through the main cell end plate and electrolyte compartment, ending about 1.5 mm from the end of the cathode.

B. Mechanical Drive System

The mechanical drive system for perturbation of the gas-electrolyte interface consists of the piston assembly in the wall of the electrolyte compartment actuated by a lever-eccentric cam mechanism, which is driven by a variable speed motor through a train of gears. The entire system, shown in Fig. 8, is set on a heavy stainless steel base of 55×30×25 cm.

The piston assembly is shown in Figs. 9 and 5. The piston itself and its surrounding cylinder consist of the plunger and needle of a microliter syringe**. The plunger, which is individually fitted with exacting precision in the stainless steel needle, is a tungsten wire of .152 mm diameter. The needle is mounted in a stainless steel cylinder of 20 mm diameter which is screwed into the cell wall. The piston is

* Baker and Adamson Reagent: Code 1969.

** Hamilton No. 7001-N.

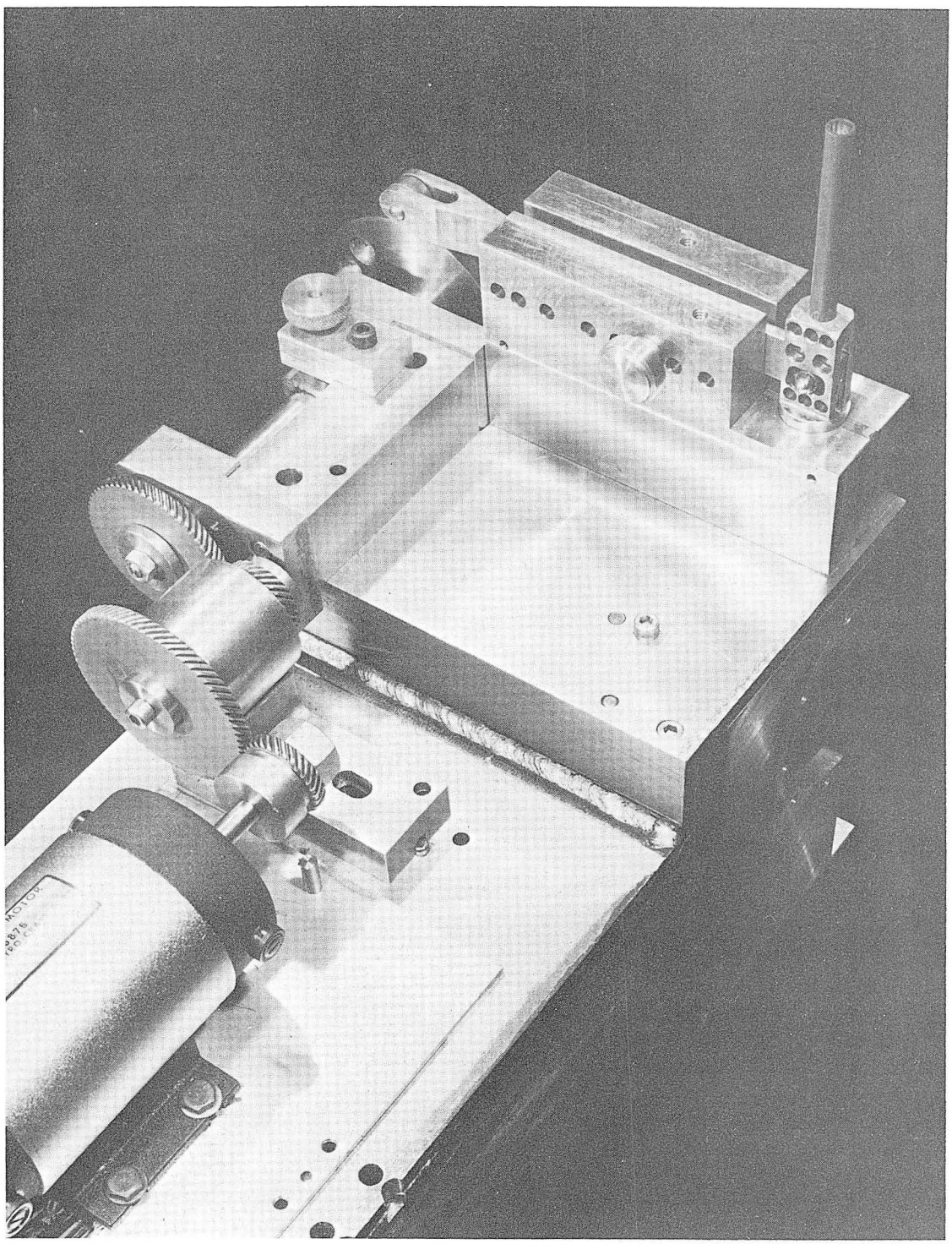

XBB 675-2736

Fig. 8 Mechanical drive system.

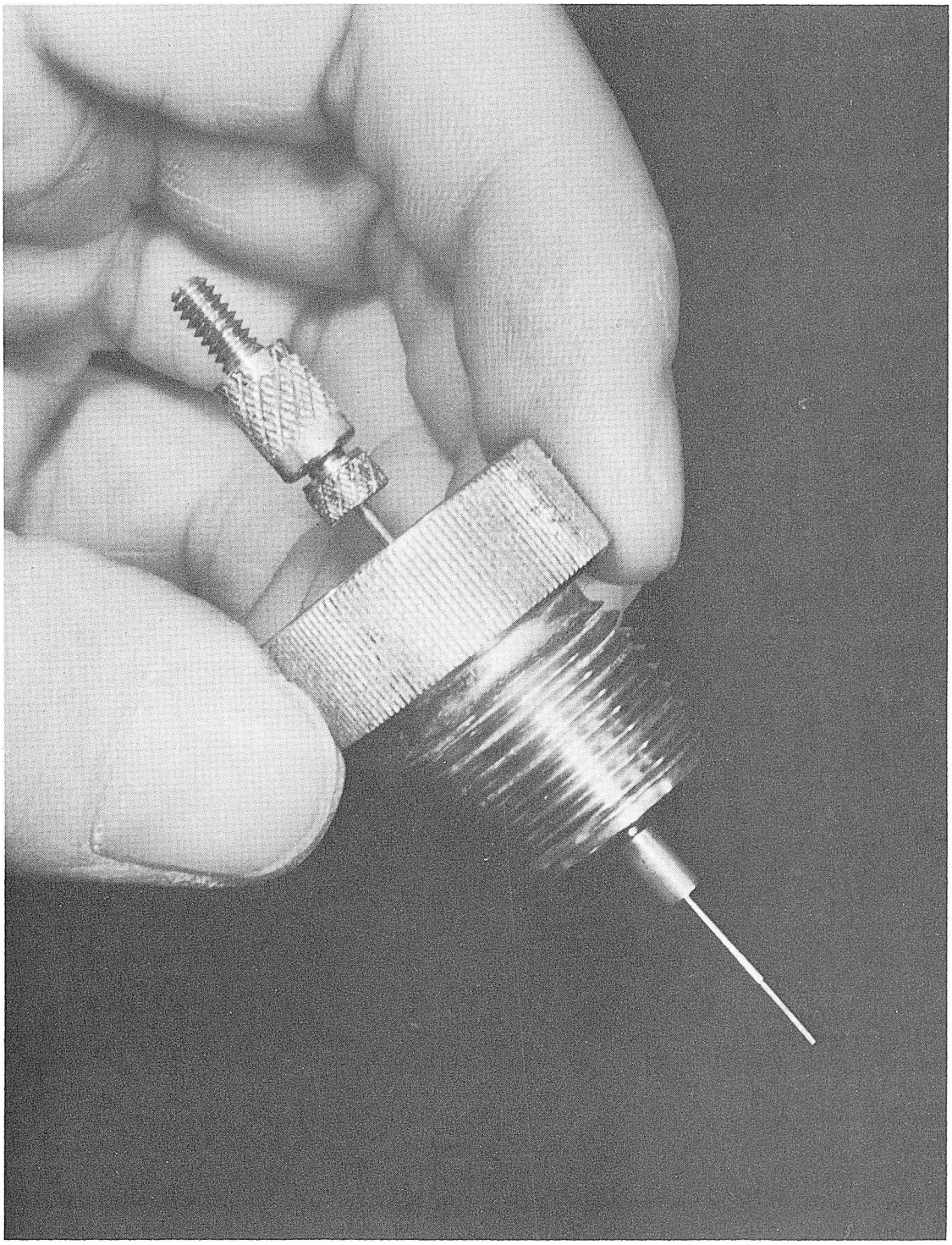

XBB 675-2732

Fig. 9 Piston assembly.

rigidly attached through a screwed fitting to the piston carrier assembly (11), which links it to the lever.

The cam, lever, and piston carrier are represented in Fig. 10. The cam (1) provides a sinusoidal displacement of the driven end of the lever (2). Two different cams have been used. Both are circular with a diameter of 90 mm, and the eccentricities of their axis are respectively, .66 mm and .2 mm. The lever pivots on a pin (5) mounted into the base. It drives the piston carrier (3) through a pin (9) firmly fixed in the lever and sliding on a polished surface in the carrier. The lever pin can be set at 8 positions to obtain various amplitudes of the piston displacement, and thus of the gas-electrolyte interface; the different amplitudes that can be obtained are given in Appendix 4. The piston carrier (3) which slides vertically into the base (4) is essentially a stainless steel cylinder of 25 mm diameter. Its upper part is cut away to accommodate the end of the lever. It has been made as light as possible by removal of excess metal to reduce the inertia of the system. The piston carrier moves downward under action of the lever and is returned by a spring (7), which thus maintains contact of the lever-wheel (6) with the cam. This spring must provide enough force to maintain contact with the cam at inertial loads encountered at relatively high frequencies but must also avoid placing excessive pressure on the cam. A spring of 18 mm diameter made of a 1.2 mm steel wire was finally used after several trials; it has a force constant of about 18×10^5 dynes/cm. A friction break device is provided on the shaft carrying the cam to reduce backlash in the gears and obtain a more uniform movement.

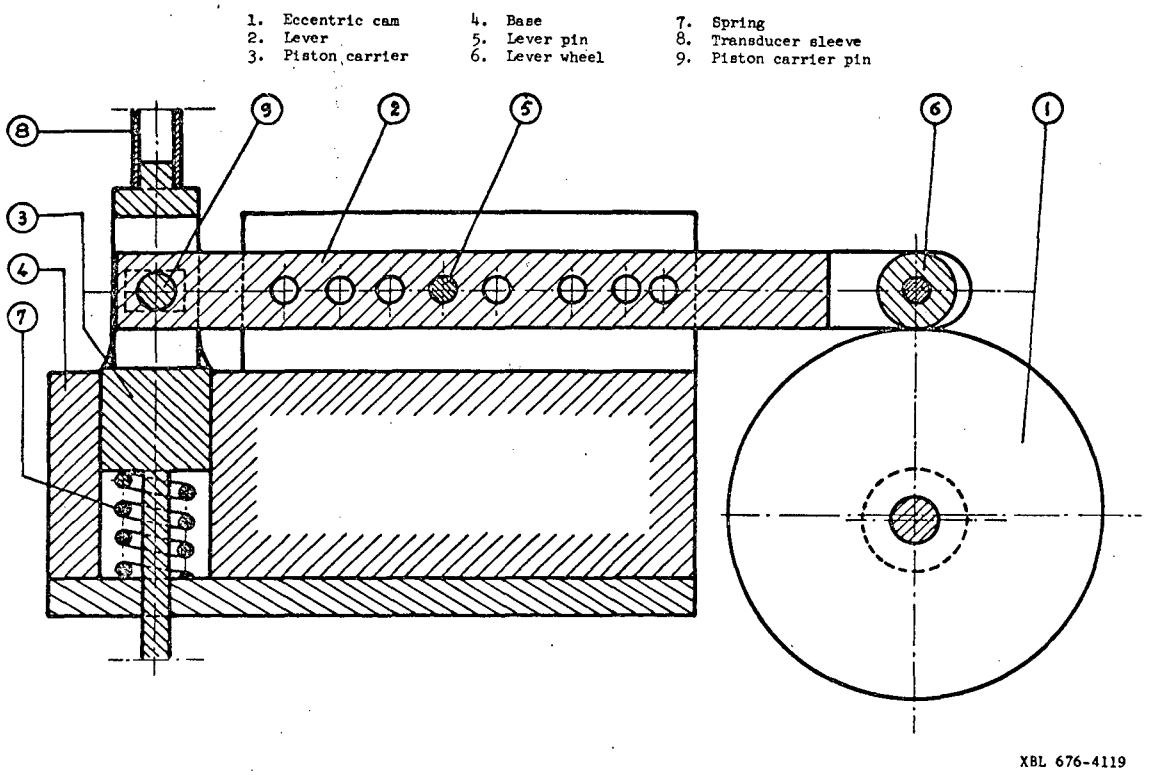

Fig. 10 Mechanical drive components.
(piston carrier, lever, and cam)

The driver for the piston mechanism is an Electro-Craft E 600-4 speed controlled DC electric motor which can provide up to 4 in./lb. torque at speeds ranging from 5 to 3,000 rpm. The controller, which includes a speed sensor and complete feedback amplifier, can maintain rotation speed constant to within ±3% and thus give a uniform sine movement to the piston. The rotational movement of the motor shaft is transmitted to the eccentric cam through a train of four Boston gears which provide a total reduction factor of 15/72. This allows a range of frequencies of the piston from 1 stroke every 8 seconds up to about 10 strokes per second. Alternative gear arrangements provide various ratios ranging up to 12/1.

C. External Electrical Circuit

The electrical circuit used during conduct of these experiments is represented in Fig. 11. It employs a constant current power supply that provides the current flowing through the cell between the silver cathode and the nickel counter-electrode. The current is measured with high accuracy by the voltage drop it creates across a resistor placed in series with the cell.

A Keithley picoampere source - Model 261 - is used as a power supply for this circuit. Its output ranges from 10^{-14} to 1.1×10^{-4} A in 8 decades. The current measuring resistor is inserted between the power supply and the cathode, as discussed in the previous chapter. A film type resistor has been chosen for its non-inductive property, and is shielded by an aluminum box; a 4.75 KΩ resistor permits measurements of all currents in the range considered. The piston is electrically connected to the counter electrode and both are held at ground potential by connection to

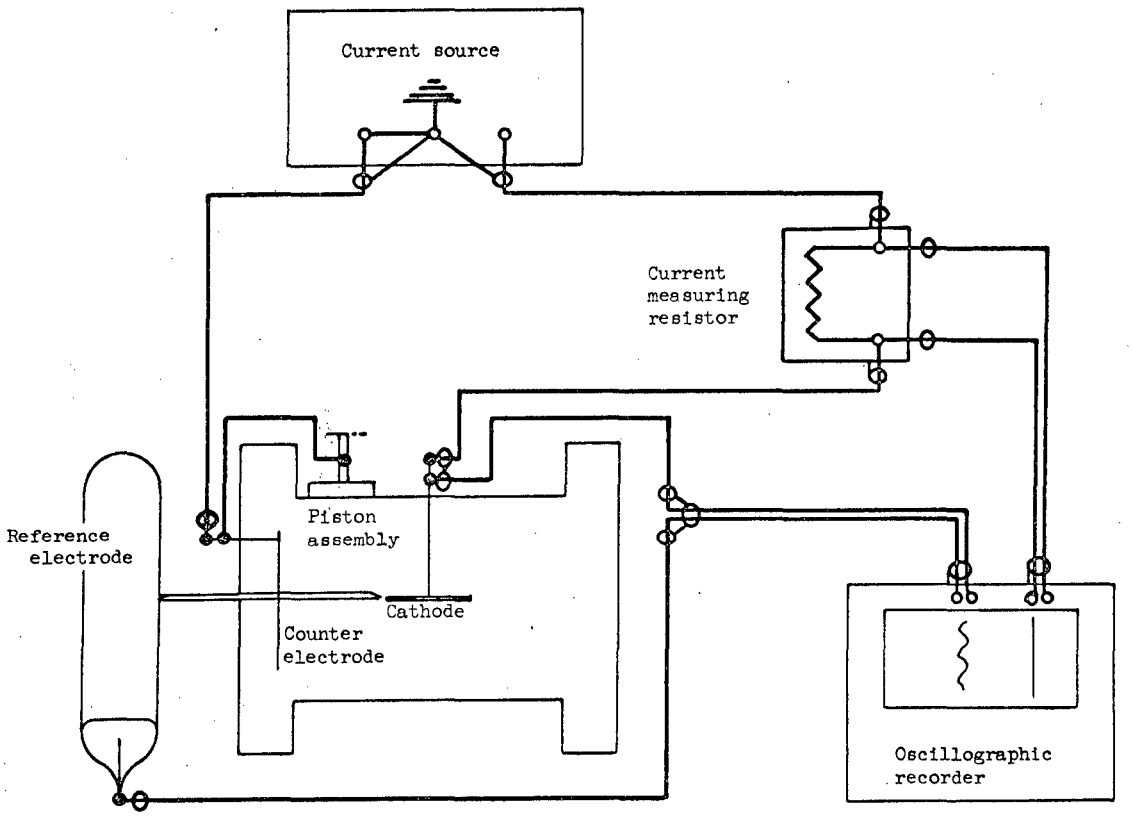

XBL 676-4120

Fig. 11 Electrical circuit.

the power supply ground terminal (power common ground). Disturbances due to any electrical field are minimized by use of shielded cables with BNC connectors. Shielding of the circuit is connected to power common ground at the power supply.

The mechanical displacement of the piston is converted by a position transducer into an electric output signal which can be recorded. The transducer used is of the linear variable capacitance type.* It employs a cylindrical dielectric sleeve, which is attached to the piston carrier, moving in the annular space between fixed capacitor electrodes. The capacitance change associated with the piston movement is detected by a 1.3 MHz bridge type driver unit which provides ±10 volts DC output linearly related to the transducer sleeve position.**

The potential drop across the current measuring resistor, the cathode-reference electrode potential difference, and the position transducer system output are simultaneously recorded on a Brush Mark 200 multichannel oscillographic recorder.*** The first two of these signals are in the millivolt range and, therefore, enter through Brush high gain DC preamplifiers Model 4215 - 10. These have calibrated zero suppression which permits use of the trace zero position to represent operation in the absence of meniscus movement and a maximum sensitivity of 100 μv per chart line. The piston position output signal from the transducer unit enters through a Brush DC preamplifier Model 4215 - 70.

---

* Lion Research Corp., C-Line Linear Variable Capacitance Transducer Model LVC 301.

**Lion Research Corp., C-Line Driver Unit - Model 202.

***Brush Mark 200 Recorder Model RF 1783-60/5 3364.

D. Systems for Filling the Cell With Electrolyte and for Gas Supply

The systems used for filling the cell with electrolyte, and for gas supply are represented in Fig. 12. The two different circuits are obtained by change of the connection (b) of valve (4) as shown on the diagram. All lines are of Tygon tubing.

The equipment used for filling the cell consists of a vacuum system and electrolyte supply vessel (1). The vacuum system, which includes two cold traps (5,6) and a mercury manometer (7), is connected to a Welch Duo Seal vacuum pump that can provide a pressure as low as 5×10^{-3} torr. Change in the position of the three-way stopcock (4) permits the degassing of the solution, the evacuation of the cell, or both at the same time. The other stopcocks represented on the right side of the round bottom flask are used for detection of any leakage. Since the electrolyte flows through the tube (3) to valves (8,9,10) during the filling of the cell, the contamination of the solution with grease is avoided by use of Teflon stopcocks.

The system is converted from electrolyte filling to gas supply by connection of the Tygon line (g) to the position (b) of valve (4) and by disconnection of valve (10). In this configuration, it includes a pressure limiting device (12), two water bubblers (13,14), a surge chamber (15), and a water manometer (16). Oxygen drawn through a standard pressure regulator from a cylinder is sparged through the water bubblers in order to saturate the gas going into the cell and thus to maintain a constant partial pressure of water vapor in the gas phase. The valve (17) permits regulation of the gas flow, and the pressure limiting device, which

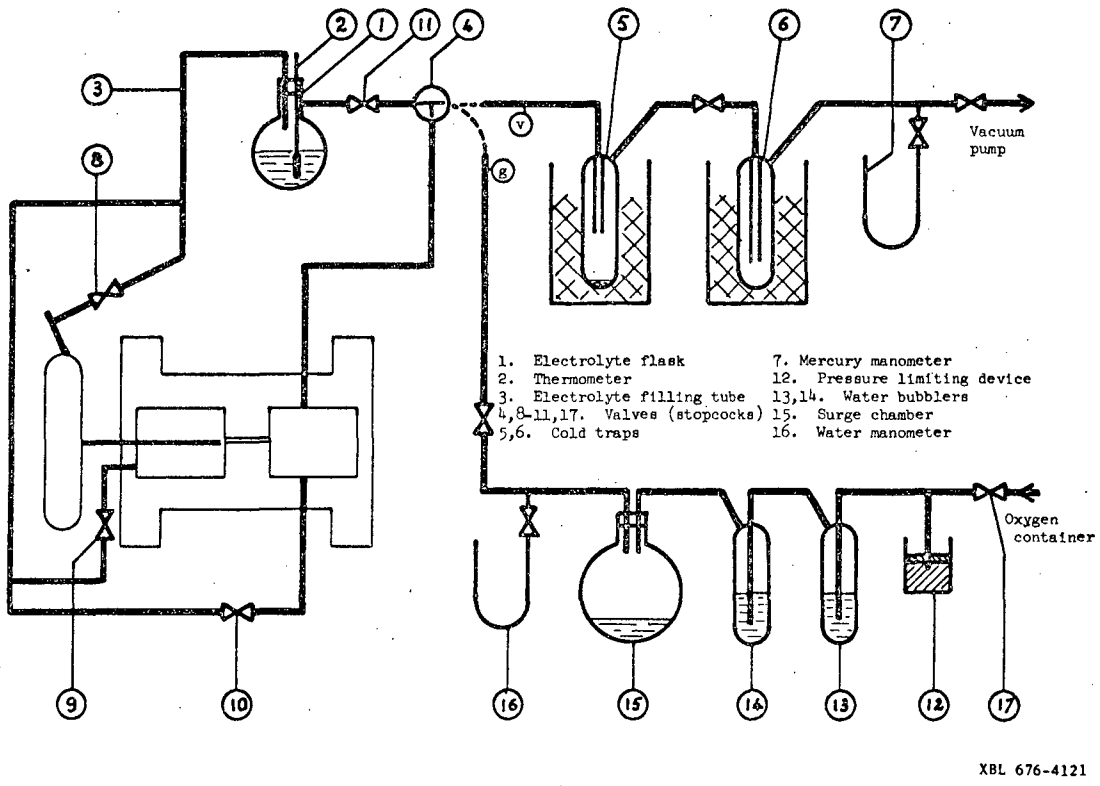

Fig. 12 Electrolyte and gas supply systems.

consists of a tube immersed 2 cm deep in mercury, keeps the gas pressure less than 78 cm of mercury absolute. The flask (15), of 1000 cm^3 volume and partly filled with electrolyte, is placed in the circuit to reduce the effect of small surges in gas supply pressure arising in the water bubblers. Any such variations of pressure can be observed by use of the water manometer.

IV. EXPERIMENTAL PROCEDURE

The nature of the experiments of this investigation allowed the examination of a wide range of displacement amplitudes and frequencies, and of currents, during a single experimental run of many hours duration. However, extensive and careful preparations were required for each such experiment. The experimental procedure can be subdivided into the preparation of the electrolyte, the filling of the cell, the pre-electrolysis, and the conduct of the measurements. These steps are described in the following sections.

A. Preparation of the Electrolyte

An approximately 2N potassium hydroxide solution was prepared by dissolution of 56g of potassium hydroxide pellets* in 500 cm^3 of distilled water whose conductivity was about 10^{-6} Ωcm. The dissolution being exothermic, the solution was cooled before degassification and titration.

1. Titration of the Electrolyte

The concentration of the solution of potassium hydroxide was determined by titration before and after each experiment. The titration could have been done by potentiometry, but a standard volumetric method gave results of good accuracy. Since potassium hydroxide is a strong base, the titration was made with hydrochloric acid, and the end-point was indicated by the change of color of methyl yellow or bromophenol blue at pH between 3.0 and 4.5.[25]

* Baker and Adamson Reagent ACS Code 2118.

The effect of dissolved carbon dioxide should be considered. In fact, carbon dioxide is always present in the atmosphere and an equilibrium concentration can be expected in the solution. Moreover, pellets of potassium hydroxide even with the purest grade contain carbonate because of superficial absorption of moisture and carbon dioxide. However, since the solution of potassium hydroxide was degassed at low pressure before the experiment, it was assumed that carbon dioxide was removed to a suitably low level before the titration.

2. Degasification of the Solution

The solution was degassed during the preparation of the cell. The procedure described below refers to the Fig. 12.

Three hundred cm^3 of potassium hydroxide solution were placed in the flask (1). The cell was isolated by the closing of the valves (8,9,10) and the switching of the three-way stopcock (4) into the position (a-b). The pressure over the solution was then reduced to about the electrolyte vapor pressure by the vacuum pump while constant agitation was maintained by use of a magnetic stirrer. To prevent damage to the vacuum pump from water vapor condensation, the two cold traps (5,6) were filled with liquid nitrogen. The temperature of the solution could be observed on the thermometer (2). If the temperature was too close to the boiling point under the reduced pressure, ebullition was avoided by the closing of valve (4). The temperature of the solution usually decreased from 23°C to 8°C during the first hour of degasification. After a period of three hours, when almost no more gas bubbles were evolved from the solution, the cell was inserted in the vacuum circuit.

B. Filling of the Cell

The cell was filled after evacuation of the cell-reference electrode system. The electrolyte was then permitted to flow into the cell driven by higher external pressure.

1. Evacuation of the Cell-Reference Electrode System

After the electrolyte was degassed, the vacuum system represented in Fig. 12 was evacuated to a pressure equal to the electrolyte vapor pressure. At this point, all the valves were open and the three-way stopcock (4) was in position (a-b-c). The stirring of the potassium hydroxide solution in flask (1) was continued throughout. During this operation, some gas bubbles could usually be seen to come out of the mercury used in the reference electrode. They frequently ejected a few small droplets of mercury with them. To avoid the risk of plugging the capillary tube with mercury or mercuric oxide from such droplets, a layer of about 1 cm thickness of water was kept above the mercuric oxide; this water evaporated almost completely under the vacuum. The entire system was held at electrolyte vapor pressure and for about six hours before the cell was filled. At that time, the electrolyte temperature was between 8°C and 12°C.

2. Procedure for Filling the Cell

To fill the electrolyte compartment of the cell with the potassium hydroxide solution, valve (11) was closed and valve (4) was turned into the position (b-c); then, the circuit was disconnected between these two valves. The glass tube (3) was immersed into the electrolyte solution and the three valves (6,7,8) in connection with the cell-reference electrode

system were closed. When valve (11) was slowly opened, the pressure in the flask was increased so that the electrolyte flowed through the tube (3) up to the closed valves. The pressure in the flask could not be higher than a few centimeters of mercury or else excessive turbulence might be created during the filling of the reference electrode that would disturb the mercuric oxide layer. Next, valve (8) was opened carefully to fill half of the reference electrode. If some mercuric oxide floated at the surface of the electrolyte, it could be removed by creation of mild turbulence in the solution. This could be done either by further opening of valve (8) or by an increase in the pressure in the flask. To avoid the risk of mercuric oxide flowing with the electrolyte through the Luggin capillary into the electrolyte compartment of the cell, the solution in the half-filled reference cell was left idle for ten minutes. Meanwhile, the electrolyte compartment was partly filled through valve (9). Then, the reference electrode was completely filled, followed by the electrolyte compartment of the cell. With the two valves (8,9) open, the electrolyte was allowed to flow through the silver capillary tube into the gas compartment. After this flow was established, valve (4) was closed and valve (10) was opened to fill the gas compartment with electrolyte. Finally, when the cell was completely filled, and with the three valves (8,9,10) open, a pressure of one atmosphere was introduced in the flask (1) by opening of valve (11).

During the filling of the cell, the temperature of the electrolyte was 10-12°C. Because of the water evaporation that occurred during evacuation, the reference electrode and the cell body were also at a

relatively low temperature. Therefore, the temperature of the system had to be allowed to reach thermal equilibrium with the laboratory ambient temperature. For this purpose, the cell was kept filled with electrolyte overnight with the three valves (8,9,10) open before proceeding with the preparation.

3. Gas Supply

After the cell had thermally equilibrated with its surroundings, the valves (8,10) were closed and the tygon tube going from the cell to valve (10) disconnected, valve (4) being closed. Then, the oxygen circuit was connected at the opening (b) of valve (4) as shown in Fig. 12. The oxygen flow was adjusted by valve (17), with the supply pressure limited to below 78 cm of mercury absolute by the mercury column (12). When the oxygen pressure in the circuit reached about 15 cm of water above the atmospheric pressure, valve (17) was closed and the oxygen flow stopped. Then valve (4) was opened, and the electrolyte that was in the gas compartment flowed slowly out of the cell. During this last operation, the oxygen pressure in the circuit decreased by about 30 cm of water, at which time flow ceased until valve (17) was opened again. Oxygen was sparged through the water bubblers at a flow of about 1.5 cm^3/sec.

Any change of pressure in the gas compartment can have a small effect on the O-ring seal such as the one around the cathode, and thus produce a change of volume of the electrolyte compartment. Consequently, there was a risk of a gas bubble being drawn through the cathode capillary tube into the electrolyte compartment. This was avoided by valve (9) being kept open during the manipulations described and being closed only after the gas compartment was empty of electrolyte.

The final step in filling the cell was the positioning of the gas-electrolyte interface by use of the adjustment screw. This screw was advanced to flood the base completely and then backed off between 12 and 15° to adjust the meniscus approximately in the middle of the tube.* A constant current of 50 μA was immediately imposed between the cathode and the counter-electrode to minimize saturation with oxygen of the cell electrolyte.

C. Pre-Electrolysis

Impurities even at extremely small concentrations can influence the polarization characteristic of the oxygen electrode, particularly at very small currents. Thus, such impurities prevent reproducible measurements and should be avoided. Since it is difficult to prepare a solution with a concentration of impurities lower than 10^{-6} mole/liter, and since impurities should be reduced to a concentration of 10^{-10} mole/liter,[26] the electrolyte is purified by a pre-electrolysis as suggested by Azzam[27] and Yeager.[28]

In this work, the pre-electrolysis was conducted in the experimental cell at the silver cathode. The constant pre-electrolysis current was passed through the cell until the difference in voltage between the cathode and the reference electrode showed no further change with time. For a current of 50 μA, which was equal to the largest value used during

* To displace the gas-electrolyte interface of 10 mm, from one end to the middle of the capillary tube, the rotation of the screw is:

$$r = 360° \times \frac{40}{25.6} \times \left(\frac{.15}{3.175}\right)^2 \times 10 \simeq 13°.$$

the measurements, it usually took 5 to 6 hours to reach a steady overpotential. However, the pre-electrolysis was conducted for about 20 hours. With such a pre-electrolysis, polarization measurements were reproducible within ±10 mV.

If the piston assembly were connected to the counter-electrode during pre-electrolysis, it would act as an anode and, since the plunger is made of tungsten, would dissolve to give tungstate ions.[29] In fact, like molybdenum, tungsten is rapidly anodically attacked in alkali solutions at low current densities.* Therefore, the piston was connected to the cathode (both were grounded) during pre-electrolysis.

D. Conduct of the Measurements

The influence of the frequency and amplitude of the displacement of the gas-electrolyte interface was investigated under galvanostatic conditions at different electrode currents. The silver capillary tube was cleaned between each experiment with a dilute solution of nitric acid and then rinsed with distilled water. However, as shown by Bonnemay[30] who took pictures of a silver plate with an electron microscope, the intergranular regions are particularly attacked after exposure of 48 hours in a concentrated solution of potassium hydroxide. Therefore, the silver cathode was stabilized before each experiment by being immersed for two days in a 2N potassium hydroxide solution and then rinsed with distilled water.

---

* Assuming that the exposed surface of the plunger is a cylinder of 152μ diameter and 5mm height, and that all the current flows from the cathode to the plunger, the current density is found to be approximately 2 mA/cm^2 which is too low a value to make tungsten passive.[29]

1. Electrode Polarization Characteristics

Experimental polarization curves were obtained by measuring the potential of the silver cathode relative to a reference electrode while a constant current was flowing through the cell. The ohmic potential drop in the electrolyte was reduced by placing the tip of the Luggin capillary close to the cathode; however, it was set at a distance equal to approximately four times the outside diameter of the Luggin capillary so as not to disturb the current flow in the electrolyte. Measurements were made for cell currents ranging from 1μA to 50μA. Polarization data were taken before, during, and after each series of measurements to check the validity of the results.

2. Investigation of the Frequency and Amplitude of the Meniscus Movement

For a given current, the influence of the frequency of the movement of the gas-electrolyte interface was investigated for various amplitudes of the displacement. Variations of the cathode voltage relative to the reference electrode were recorded simultaneously with the piston movement and the current flowing through the cell.

The cathode voltage was studied for frequencies of the meniscus movement ranging from about .25 cycles/sec to about 5 cycles/sec for a given current and displacement amplitude. This was done by control of the motor speed. Measurements were made for five or six different frequencies, starting at the lowest value and increasing to the highest; then, as a check, another measurement was made at a low frequency of about .5 cycles/sec.

The influence of the frequency was investigated for at least four amplitudes of the meniscus displacement ranging from .35 mm to 3.5 mm. This involved changing the position of the lever pin as discussed in the previous chapter. For a given current, measurements were made from the smallest amplitude to the largest one. Amplitudes ranging between .1 mm and .35 mm were obtained in a separate series of measurements by use of the cam with smaller eccentricity.

The effects of the frequency and amplitude of the meniscus movement were investigated for currents ranging from 5μA to 50μA. Since polarization data were taken during experiments for currents between 1μA and 50μA, the sequence in which the currents were investigated should not matter. In most cases, measurements were made for currents increasing from the lowest value to the highest one.

The record of an experimental run consists of an annotated oscillographic recorder chart which has traces of the cathode voltage, piston transducer output, and voltage drop across the current measuring resistor. It also includes timing marks at one second intervals.

V. RESULTS AND DISCUSSION

The intent of these experiments was to investigate the effects of the periodic displacement of the gas-electrolyte interface of a film type porous gas electrode. Four experimental series measuring these effects were completed and are reported in the next section of this chapter. However, the interpretation of the results of these experiments indicates that the conditions existing in the capillary gas electrode of the experiment deviated significantly from the design conditions and the results must be viewed with this in mind. Nevertheless, these results can give a qualitative indication of effects to be found with meniscus movement and provide a partial verification of the expectations discussed in the introduction of this work. A further series of experiments involving the capillary gas electrodes without meniscus movement was undertaken to determine the source of problems found in the experiments with meniscus displacements. These are also discussed at length in this chapter.

A. Effects of the Meniscus Movement

A total of four experimental series are reported in this section. All were conducted generally according to the procedure described in the previous chapter, although in detail it represents the most recent experimental procedure. The conditions of the different experiments differed essentially by the length of pre-electrolysis of the potassium hydroxide solution. The four experiments were conducted at room temperature equal to 23.5°C, with an electrolyte concentration about 2N (between 1.80N and 2.05N). In these experiments, expected meniscus displacements from .08mm to 2.64mm were investigated at frequencies ranging

from about .2Hz to 45Hz and currents from about 5μA to 45μA. The conditions for each experimental series are summarized in Table 1.

Table 1

Summary of Experimental Conditions

Experiment Number	Electrolyte Concentration (mole/liter)	Length of pre-electrolysis (hours)	Currents Investigated μA
1	2.03	6	20.4 - 29.3
2	2.05	6	9.6 - 28.7
3	1.92	24	9.8 - 29.5
4	1.80	20	5.1-9.7-20.5-28.9-46.8

The potential/current relationship for the cathode (vs the reference electrode) in absence of meniscus displacement was determined before, during, and after each measurement as discussed in the previous chapter. These overpotential curves were found to be reproducible within a good approximation for a given experiment, as shown in Fig. 21. According to the procedure described, the meniscus was adjusted in an attempt to keep it approximately in the middle of the capillary tube. The cathode potential relative to the mercury/mercuric oxide reference electrode at very low currents is about - 30mV while the calculated reversible potential is +303mV on this scale. However, the reversible potential is almost never observed for the oxygen cathode and the former value corresponds to the results obtained by Bennion[12] who worked with the same system oxygen-silver-potassium hydroxide, as well as those by many other investigators.

The periodic response of the cathode potential relative to the reference electrode was recorded simultaneously with the piston movement and the current, as shown in Fig. 13. The left side of the trace recorded for the piston movement corresponds to the lowest position of the plunger into the electrolyte compartment, and thus to the meniscus position nearest the gas side of the capillary tube. For the overpotential curve, increasing overpotentials are represented by trace displacement to the right. The response recorded for the cathode potential relative to the reference electrode is a periodic signal of same frequency as the piston movement. However, the potential response was not sinusoidal and a phase lag, depending on the piston frequency, was usually observed. The amplitude of the electrode potential response was found to decrease with increasing frequencies and increase with increasing meniscus displacements for a given current, as shown in Figs. 14-19. In all these experiments, during the periodic movement of the gas-electrolyte interface the cathode average overpotential (mean value of periodic response) never varied more than a few millivolts (maximum of 10mV) from the value obtained in absence of meniscus movement.

During the first experimental series reported in this section, the signal recorded for the cathode potential response presented a peculiarity as shown in Fig. F1 in Appendix F. On the basic periodic response curve of the cathode potential relative to the reference electrode was superimposed a second peak always in phase with a small irregularity in the piston movement. The effect was much greater at low frequencies and disappeared at higher frequencies, as shown in Fig. F1. This suggested that the electrode overpotential was sensitive to a very small displacement of the meniscus when at a position corresponding to a reversal in

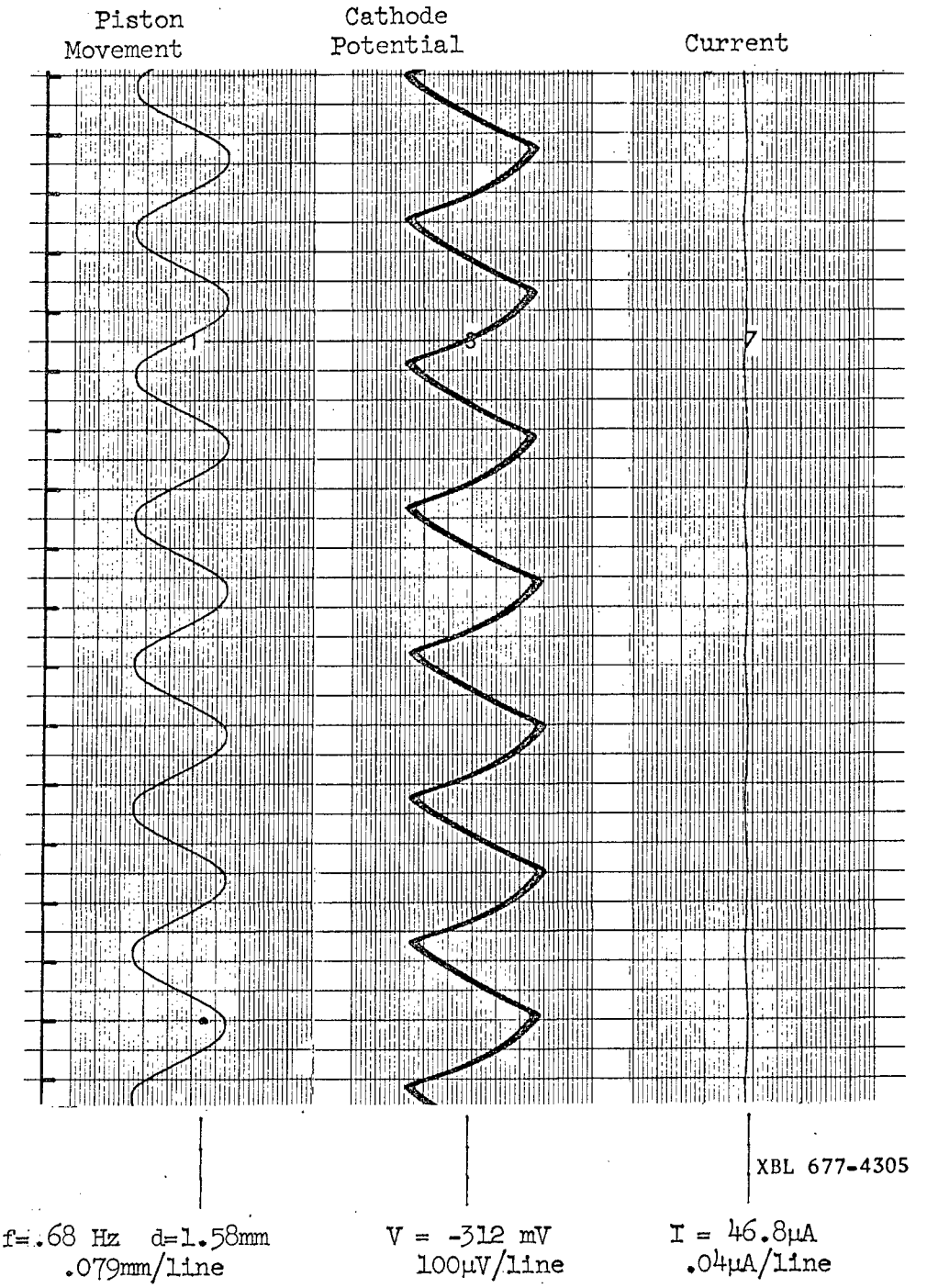

Fig. 13 Oscillographic recorder traces for piston displacement of 1.58mm, frequency of .68 Hz, and current of 46.8μA. Experimental Series No. 4.

displacement direction. It was found that this irregularity in piston movement was caused by a roughness on the surface of the piston carrier where the piston carrier pin slides. Correction of this condition (by polishing the surface of contact and use of grease in order to reduce the friction) led to a very nearly sinusoidal piston movement and to a more regular cathode potential response, as shown in Fig. 13.

During the second experimental series, the signal obtained for the cathode potential relative to the reference electrode appeared always in phase with the piston movement at any frequency and amplitude. Moreover, the potential response curve was much more sharply peaked than in most other experiments. In view of the conditions actually existing in the electrode as determined later, this apparently was the result of the nature of the meniscus shape located at the extreme gas end of the electrode.

The results obtained in the other experimental series can be considered characteristic of the effects of the periodic movement of the meniscus in the equipment as used. The amplitude of the cathode potential response was found to decrease as the frequency increased for a given amplitude at a fixed current. Greater effects were observed at higher meniscus amplitude displacements. The results obtained for piston displacements ranging from .26mm to 2.64mm for five currents ranging from 5.1μA to 46.8μA are shown in Figs. 14-19. During the last experiment, the amplitude of the cathode potential response was also investigated at different currents for a given frequency and piston displacement; the record of a run for a small piston displacement of .08mm is shown in Fig. F8 in Appendix F and the results obtained are plotted in Fig. 20. Finally, it was also found that the phase lag between the piston movement and the cathode potential response in-

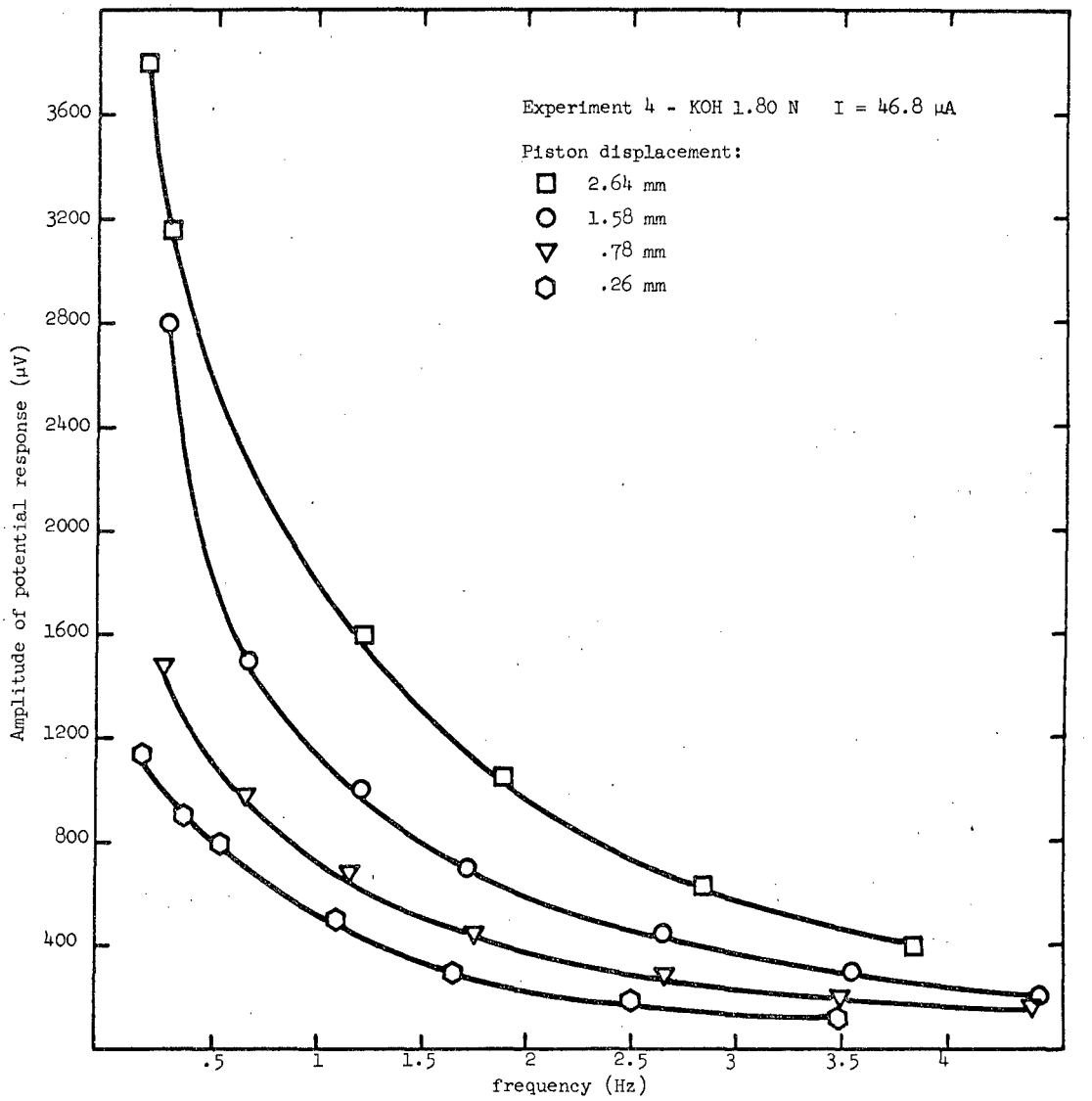

XBL 677-4322

Fig. 14 Amplitude of the cathode potential response vs frequency for a current of 46.8μA. Experimental Series No. 4.

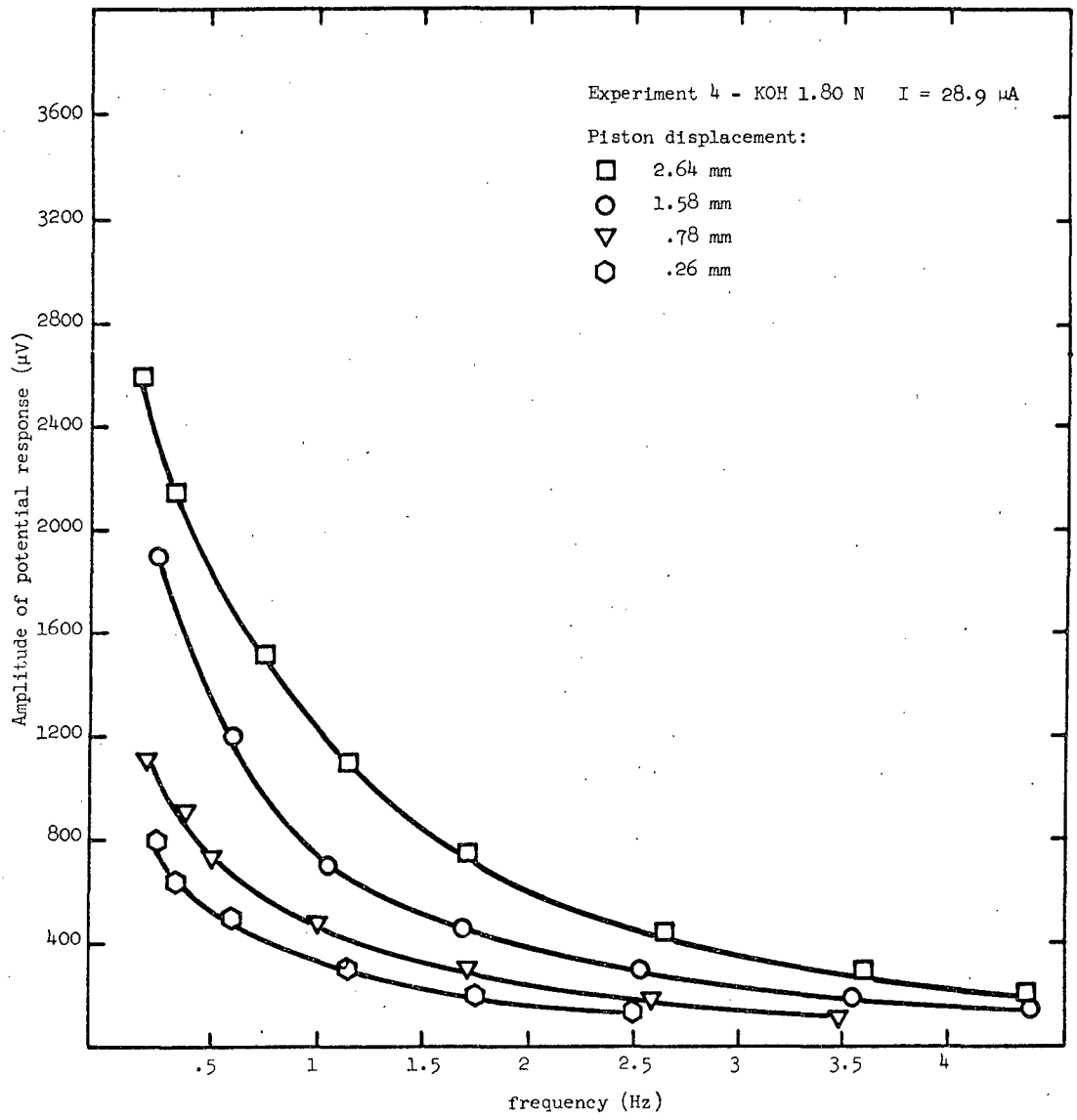

XBL 677-4316

Fig. 15 Amplitude of the cathode potential response vs frequency for a current of 28.9μA. Experimental Series No. 4.

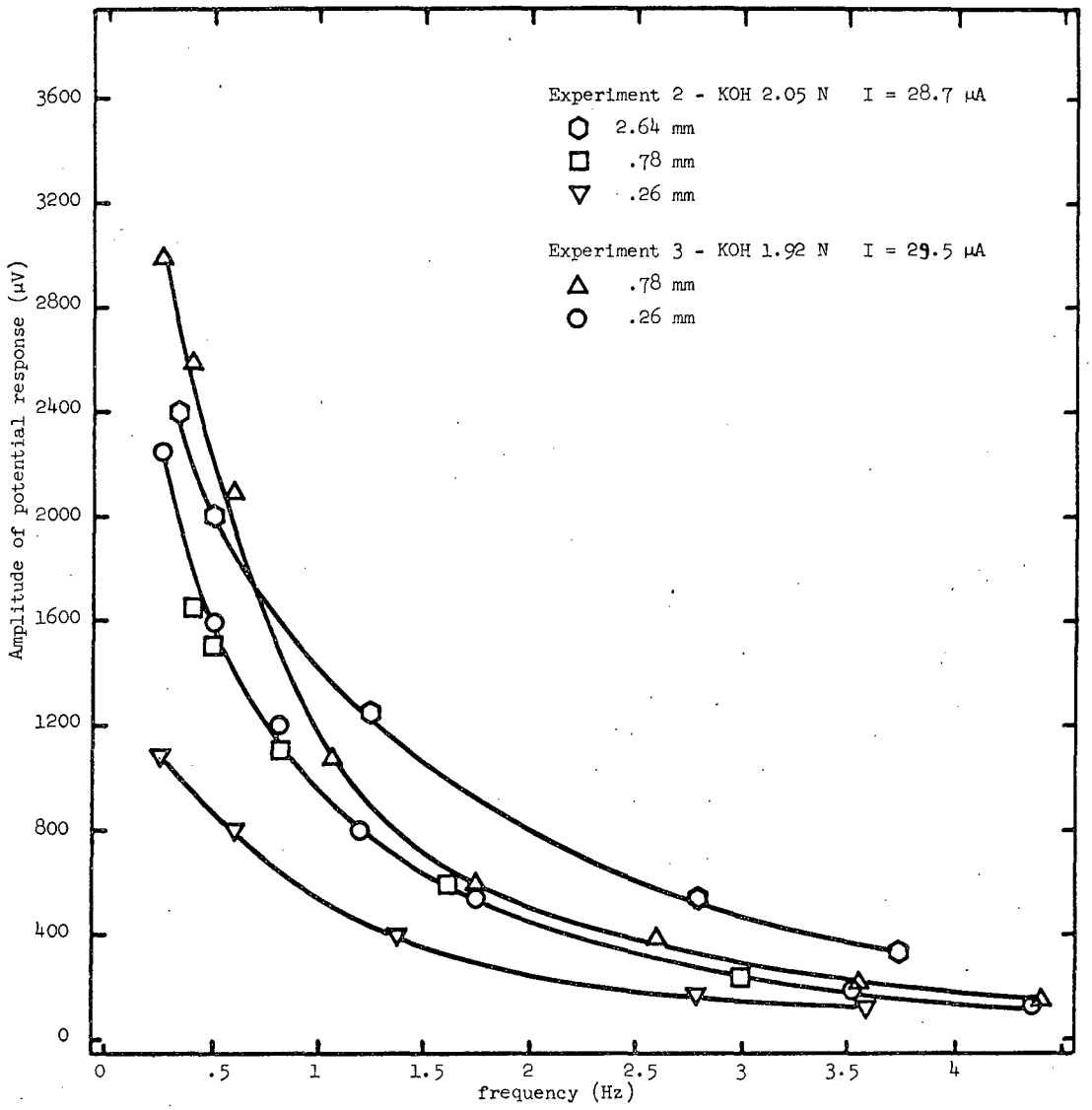

XBL 677-4319

Fig. 16 Amplitude of the cathode potential response vs frequency for currents of 28.7μA and 29.5μA. Experimental Series Nos. 2 and 3.

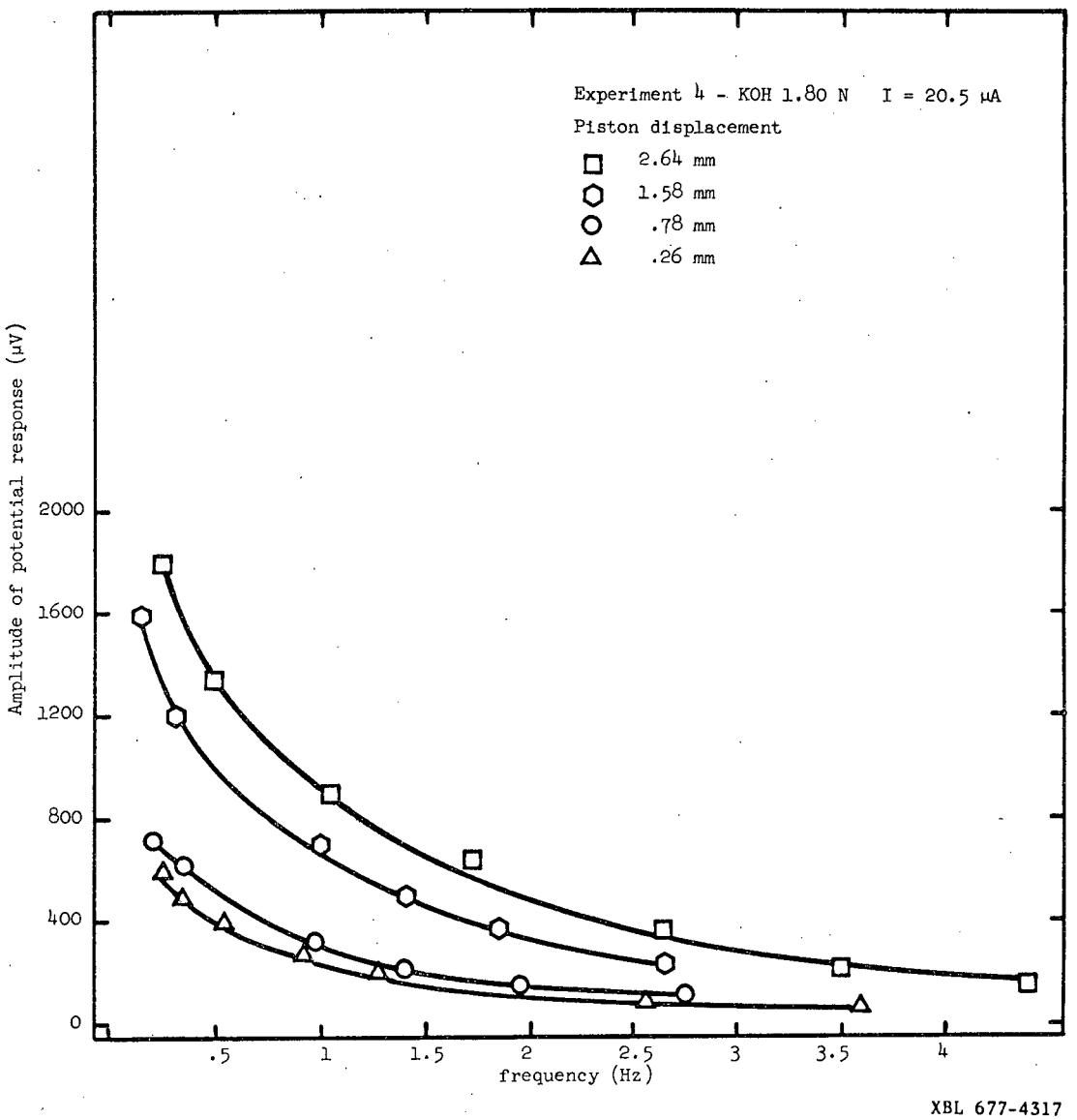

Fig. 17 Amplitude of the cathode potential response vs frequency for a current of 20.5μA. Experimental Series No. 4.

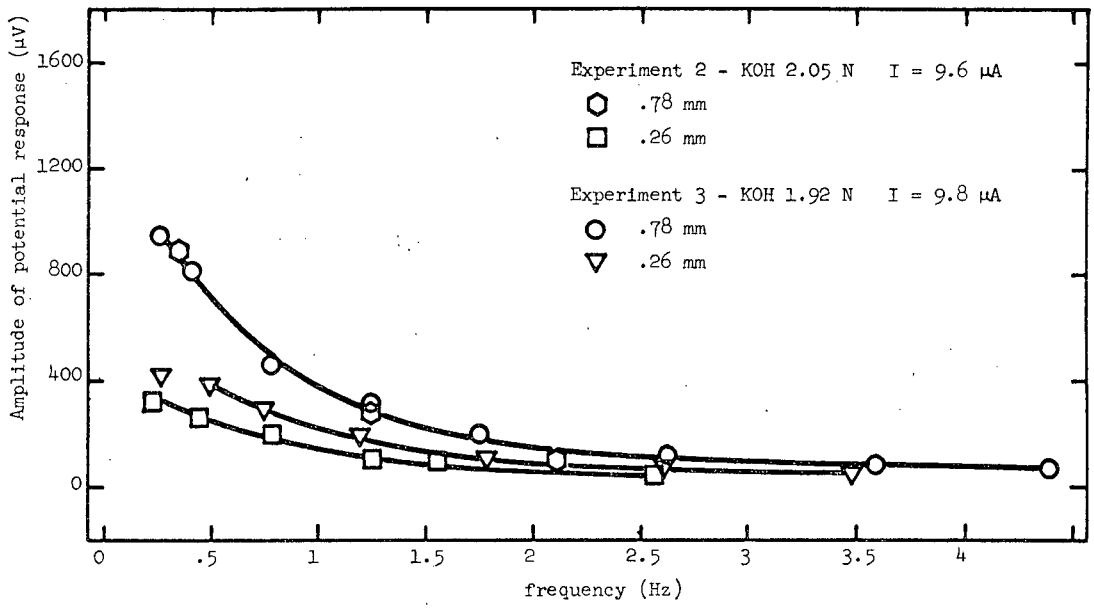

Fig. 18a

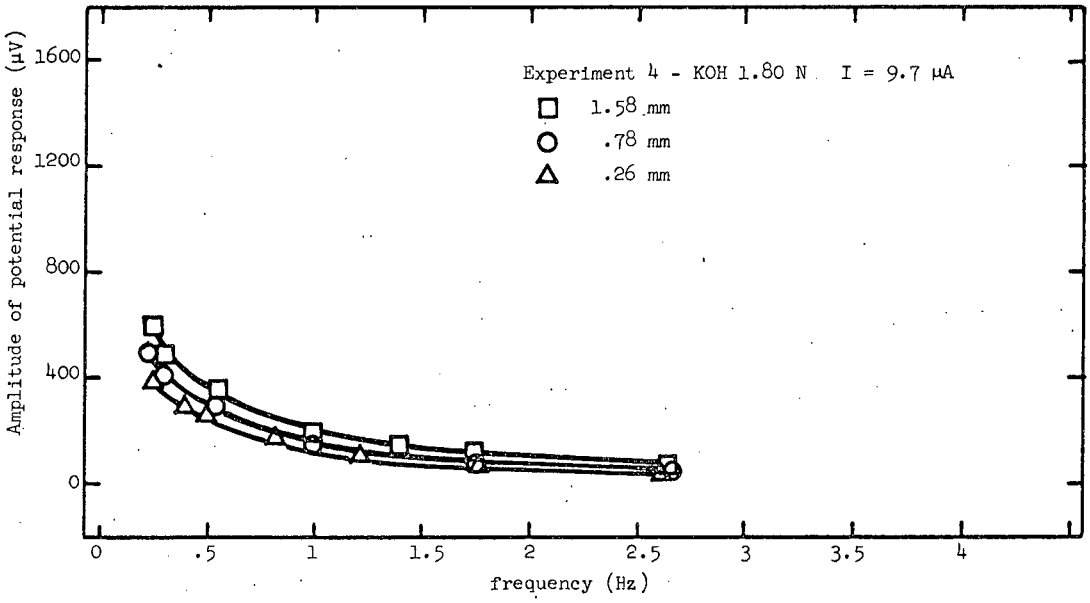

Fig. 18b

XBL 677-4320

Amplitude of the cathode potential response ve frequency for currents of 9.6μA, 9.8μA, and 9.7μA.

Experimental Series Nos. 2, 3, and 4.

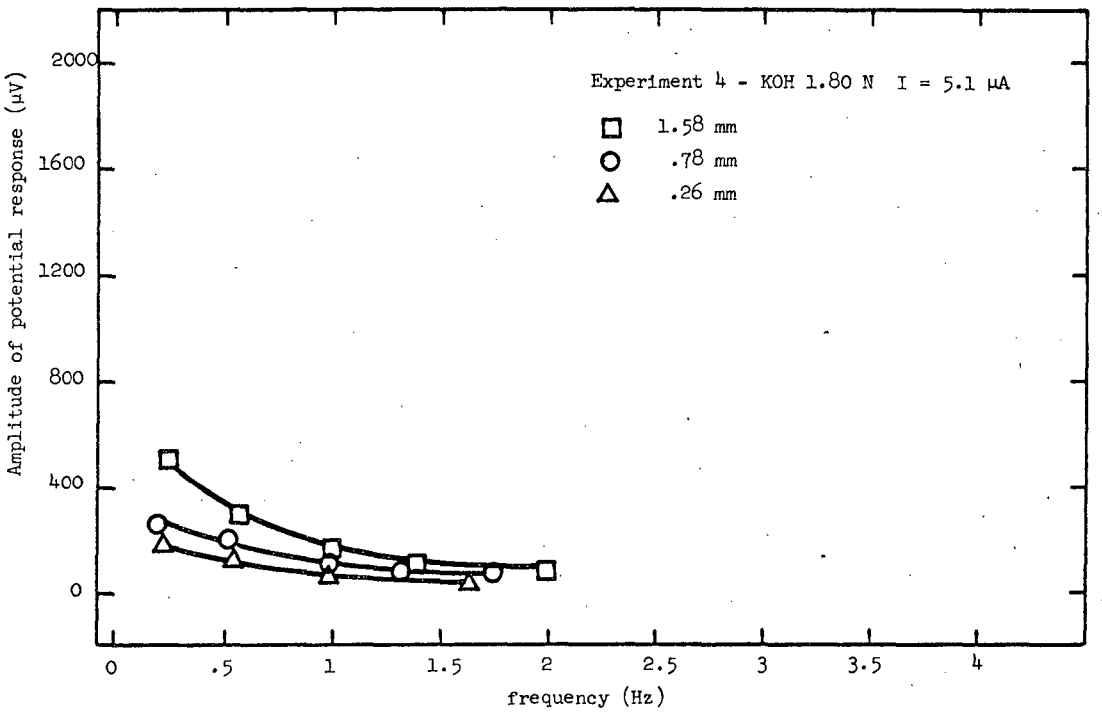

XBL 677-4318

Fig. 19 Amplitude of the cathode potential response vs frequency for a current of 5.1μA. Experimental Series No. 4.

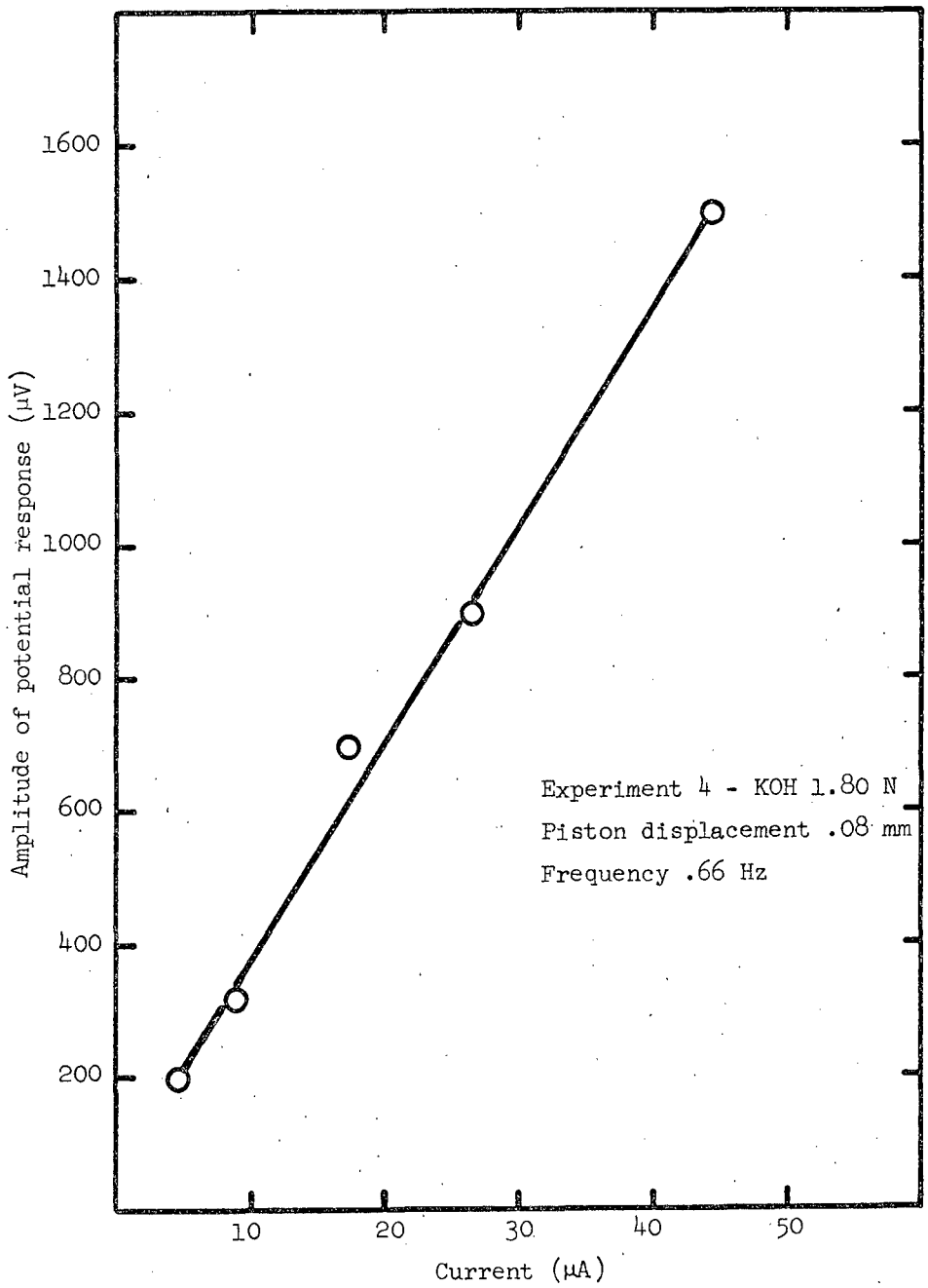

XBL 677-4321

Fig. 20 Amplitude of the cathode potential response vs current for a frequency of .66 Hz and .08mm piston displacement.

Experimental Series No. 4.

creased with increasing frequencies of the movement, as shown in Figs. F2-7 in Appendix F.

All the curves shown in Figs. 14-19 present about the same shape. However, it can be seen in Figs. 15 and 16 that measurements were not reproducible between experiments 2, 3, and 4. Figures 18a-18b also show this characteristic. All the results seem to be more coherent at frequencies higher than 2 hZ. Here the amplitude of the cathode potential response does not vary much with the amplitude of the piston displacement at a given current.

During most of the experiments it was found that at low frequencies, and in most cases for piston displacements greater than .78 mm, the signal recorded for the cathode potential response could be different from the one shown in Fig. 13. In fact, a second peak could be observed during each cycle, as shown in Fig. F9, in Appendix F. The amplitude of this second peak was found to decrease with increasing frequencies. Moving the meniscus toward the electrolyte end of the capillary tube by use of the meniscus positioning device had the effect of temporarily suppressing this irregularity in the signal; it usually returned after a short time. The amplitude of such a signal for the cathode potential response was always smaller than in the case of a response closely approximating a sine curve. This phenomenon suggested the possible location of the meniscus at the extreme gas end of the capillary tube.

In all these experiments, currents larger than any expected values (perhaps 5μA as shown in Appendix C) were passed through the cell in order to obtain measurable effects of the meniscus movement (no significant periodic response was obtained for a current of 1μA). Especially the maximum currents used were considerably larger than a pore of this size

should be able to support. Moreover, the polarization data represented in Fig. 21 (for experiment 4) show a quite low cathode potential relative to the reference electrode for such high currents. In fact, for a current of 40μA, the ohmic voltage drop through a flooded capillary tube of 150μ is 1.3 volt, as calculated in Appendix E, while the difference of voltage between the cathode and the reference electrode was only .3 volt. This suggests a much lower resistance of the electrolyte path than should be expected. The irreproducibility of the measurements of the cathode potential response, the necessity for high currents, and the low ohmic voltage drop indicated that the electrode was not performing in the manner expected. Therefore, further experiments were conducted in which the electrode overpotential was investigated without meniscus movement.

B. Existence of an Electrolyte Short Circuit Path

To investigate the low resistive component of the cathode overpotential, observed clearly at high currents, measurements of the cathode voltage relative to the mercury/mercuric oxide reference electrode were made for the meniscus located at the extreme ends of the capillary tube. This involved moving the meniscus adjusting screw in order to displace the location of the gas-electrolyte interface from one end of the tube to the other between each measurement. The difference between the two electrode potentials obtained in this way for a given current gives an approximate experimental value of the ohmic voltage drop through the electrolyte filled part of the capillary tube. Results of these measurements are reported in Table 2. Comparison of the cathode polarization characteristics represented in Fig. 21 and those given in Table 2 show that all the results obtained during the four experimental series described previously correspond to the meniscus located at the extreme gas end of the

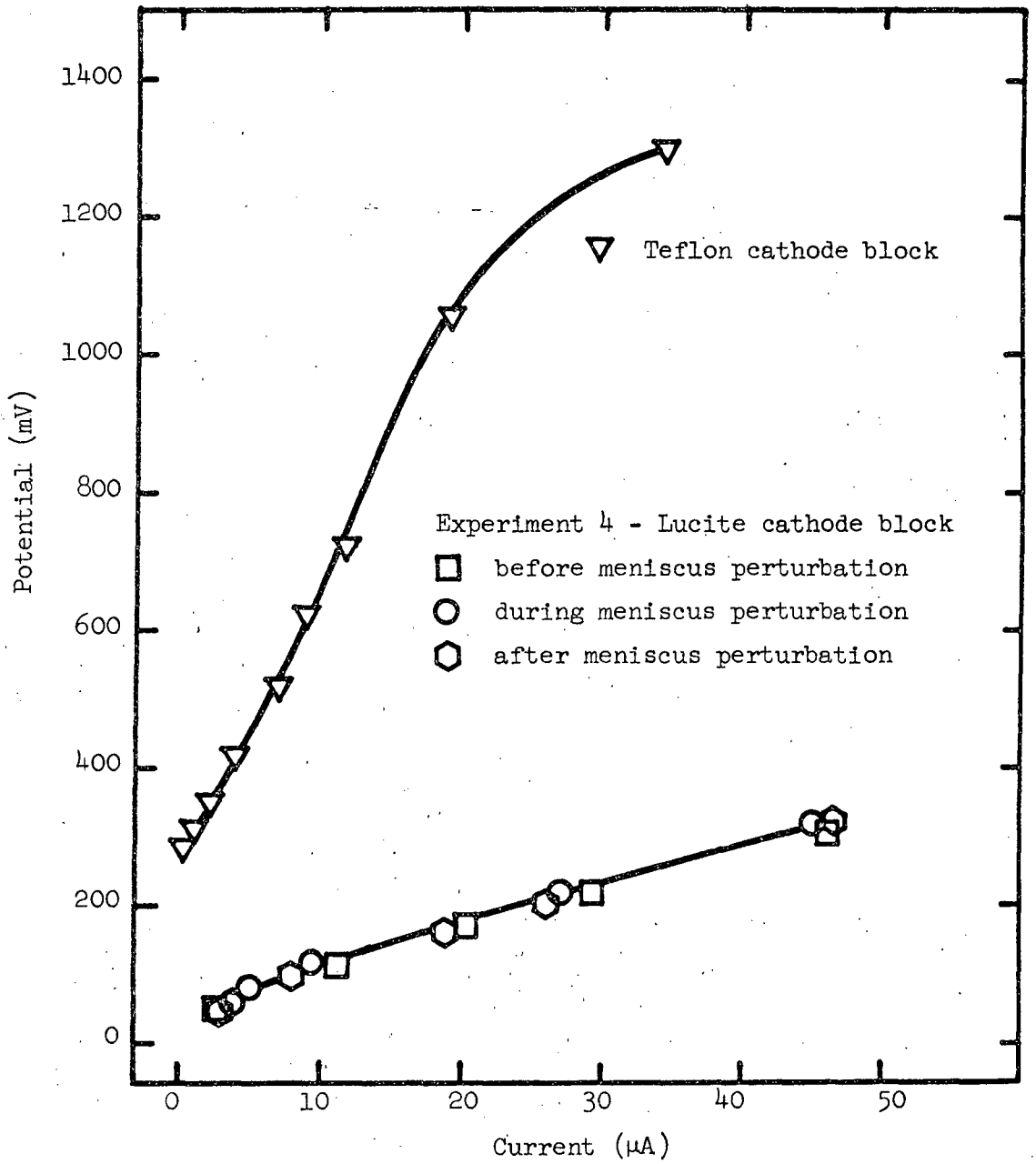

XBL 677-4323

Fig. 21 Cathode potential/current characteristics for lucite and teflon cathode block. (Cathode potential measured relative to the Hg/HgO reference electrode.)

Table 2

Oxygen Cathode Potential/Current Behavior for Lucite Cathode Block

Meniscus at gas end	Current (μA)	2	5	8	11	20.5	27	45
	Cathode Potential vs Hg/HgO Reference Electrode (mV)	-30	-80	-105	-120	-170	-220	-320
Meniscus at Electro-lyte end	Current (μA)	5	10	16	26	44		
	Cathode Potential vs. Hg/HgO Reference Electrode (mV)	-44	-56	-106	-156	-228		

capillary tube. These results also confirm a lower resistance for the ionic current path that should be expected (2.9 kΩ instead of 32 kΩ), which suggests the existence of a second electrical path in parallel with the one through the electrolyte filled part of the capillary tube. This could be the case of a thin film of electrolyte covering the cathode block and passing under, or over, the O ring seal, as shown in Fig. 22a. In fact, the external diameter of this block is so much greater than the inside diameter of the capillary tube that even a very thin film bypassing the O ring seal would offer a lower resistance. This spurious path for ionic species would explain the small ohmic drop measured across the

electrolyte filled part of the capillary tube, which is about 10 times smaller than the value calculated in Appendix E. Such a parallel path should lead to an ohmic voltage drop that would first increase and then decrease as the meniscus is moved from the gas end to the electrolyte end of the capillary tube. The current should flow primarily through the spurious path until its resistance would become larger than the resistance of the electrolyte filled part of the electrode, then largely through the electrolyte in the capillary tube. The resistance of this spurious electrolyte circuit should increase rapidly as the meniscus is moved away from the extreme gas end of the capillary tube because of the small thickness of the electrolyte film above the meniscus that would constitute a part of this path. Thus, the total resistance of the two parallel paths would increase under initial displacement of the gas-electrolyte interface from the gas end. As the interface would approach the electrolyte compartment end of the pore, the resistance of the circuit through the electrolyte in the capillary tube would become quite low and the effective resistance, and thus the overpotential, would again decrease. However, the record of the cathode potential relative to the reference electrode, during displacement of the gas-electrolyte interface from the gas end to the electrolyte end of the capillary tube shows continuous decrease in overpotential.

The behavior noted above could mean that the reaction was taking place at two places: under the electrolyte film above the meniscus in the pore as expected, and under a film covering the external surface of the silver tube that was exposed at the gas end of the lucite block. The relative importance of these reactions would depend on the respective resistance of the two competitive circuits with the spurious reaction at the end of the tube adding a sizeable increment of current to

that due to the desired reaction in the pore. Since it is likely that the resistance of the electrolyte short circuit path was different from one experiment to another, the current, passing through the electrolyte filled part of the capillary tube for the same imposed current, and thus the effects of the periodic movement of the meniscus could also vary from one experiment to another. This would explain the irreproducibility of the measurements and why such high currents could be used, and, in fact, had to be to observe a periodic response for the cathode overpotential.

It was also found that it is very difficult to measure the cathode potential relative to the reference electrode with the interface just at the end of the capillary tube in the electrolyte compartment. In fact, each time a gas bubble appeared at the tube end during such measurements, either it separated quickly into the electrolyte compartment or retreated inside the capillary tube. When a bubble could be stopped for longer than a minute, changing the current usually made it separate from the capillary tube and go into the electrolyte compartment. This might be explained by a change of interfacial tension at the electrolyte-metal interface. The record of the cathode voltage relative to the reference electrode also showed that the meniscus was not remaining at the electrolyte end of the capillary tube, since the electrode potential was increasing regularly until it reached a value corresponding to the meniscus located at the gas end of the tube. This observation is in accord with the fact that sometimes it was difficult to draw a bubble through the capillary tube, even by moving the meniscus adjusting screw enough to displace a volume of liquid 10 times greater that the inside volume of the capillary tube. One possible explanation of this effect was the existence of a certain amount of electrolyte adjacent to the

cathode block in the gas compartment as shown in Fig. 22a. In that case, attempts to adjust the meniscus away from the gas end had no other ultimate effect than drawing some potassium hydroxide solution from this source at the end of the capillary tube. The existence of such a volume of electrolyte was actually observed later. It also explains why a fast displacement of the meniscus adjusting screw could draw an oxygen bubble through the capillary tube while a slow rotation could not, and why the meniscus could move from the electrolyte end to the gas end of the capillary tube by itself.

The hypothesis suggested above could be verified experimentally by suppression of the spurious ionic current path. In such case, the current would flow entirely through the electrolyte in the pore as expected in the experimental design. The way selected to avoid the spurious path for ionic species was to use a cathode block made of a material, teflon, that would not be wetted by the electrolyte. Also, it was necessary to modify the shape of the cathode support to avoid the existence of a volume of potassium hydroxide solution retained by capillary forces. This was done as shown in Fig. 22b.

C. Overpotential Measurements with Teflon Cathode Block

Experiments with the cathode set in a teflon block were limited to overpotential/current measurements taken without meniscus displacement because such data were sufficient to justify the hypothesis discussed previously and because they revealed other factors that still prevented achievement of the design conditions for the electrode. This investigation was concerned with the ohmic voltage drop in the electrolyte filled part of the capillary tube and with the overpotential characteristics of the electrode.

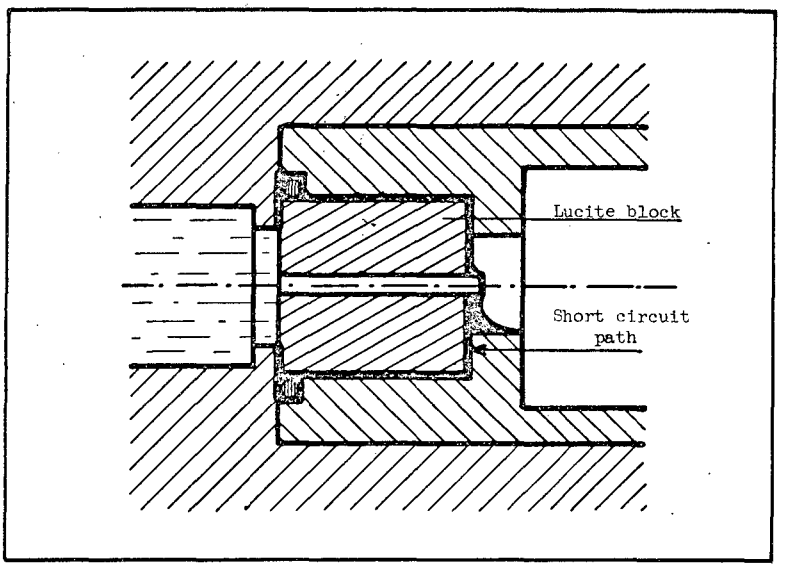

Fig. 22a Diagram illustrating electrolyte short circuit path.

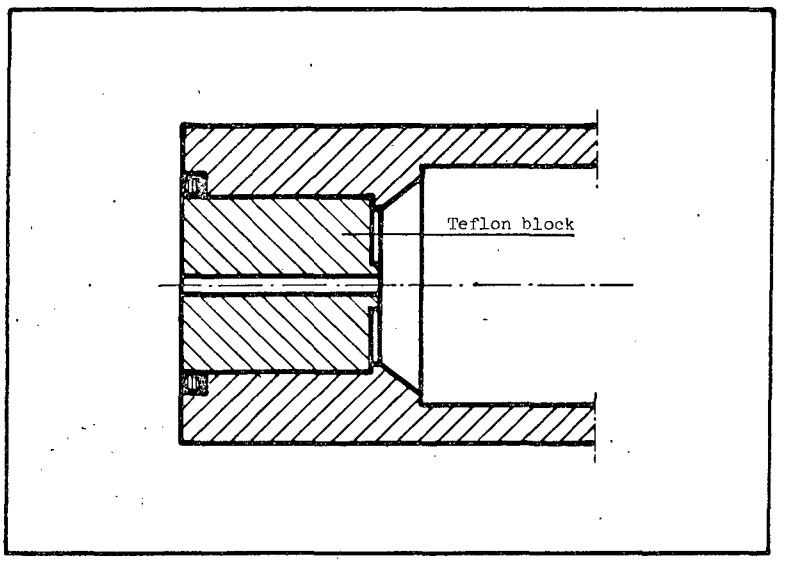

XBL 677-4324

Fig. 22b Modifications to the cathode mounting and cathode carrier.

The polarization data for the meniscus located at the gas end of the capillary tube taken during two experiments which gave about the same results are plotted in Fig. 21. The cathode voltage relative to the reference electrode was found to be much larger with the teflon block than with the lucite block. Other measurements were made for the meniscus located at the electrolyte end; results are shown in Fig. 23. Experimental values of ohmic voltage drop across the electrolyte filled part of the capillary tube determined from these results are of the order of magnitude expected. For a high current of 20μA, the difference between the polarization measurement, for the meniscus located at both ends is 920 mV, which corresponds to a resistance of 46 kΩ. However, the potential measurements obtained at vanishing currents vary from the results previously obtained for the lucite cathode block (-280mV instead of -30mV). Since near zero current conditions the cathode potential relative to the reference electrode should have about the same value in all cases, and since this value should be of the same order as that normally found for oxygen on silver (about -50 mV[12]), it appeared that the electrode reaction characteristics differed for the two ends of the capillary tube. To investigate this, the electrode was installed in the cell with the former gas end now serving as the liquid end and a further series of overpotential measurements was conducted. The overpotential curves obtained for this arrangement, both for the meniscus at the "new" gas end and the "new" liquid end of the electrode, are given along with those for the "old" configuration in Table 3 and are plotted in Fig. 23.

They show entirely different electrode kinetic behavior for the two ends of the silver capillary tubes. This indicates differences in the form or surface condition of the inner surface of the capillary tube

Table 3

Oxygen Cathode Potential/Current Behavior for Teflon Cathode Block

Electrode Normal Position

Meniscus at gas end	Current (μA)	.5	1	2	4	7	11.5	19	34.5	
	Cathode Potential vs Hg/HgO Reference Electrode (mV)	-290	-310	-350	-415	-520	-725	-1060	-1300	
Meniscus at electro-lyte end	Current (μA)	.5	1	2	9	7	10	15	20	25
	Cathode Potential vs Hg/HgO Reference Electrode (mV)	-10	-20	-34	-50	-60	-80	-100	-125	-150

Electrode Reversed Position

Meniscus at gas end	Current (μA)	.5	1	2	3	4	7	10	16	20	30
	Cathode Potential vs Hg/HgO Reference Electrode (mV)	-30	-52	-90	-120	-370	-800	-960	-1150	-1250	-1350
Meniscus at Electro-lyte end	Current (μA)	.5	1	2	3	4	7	10	15	20	30
	Cathode Potential vs Hg/HgO Reference Electrode (mV)	+50	+40	+20	+5	-15	-70	-120	-190	-280	-570

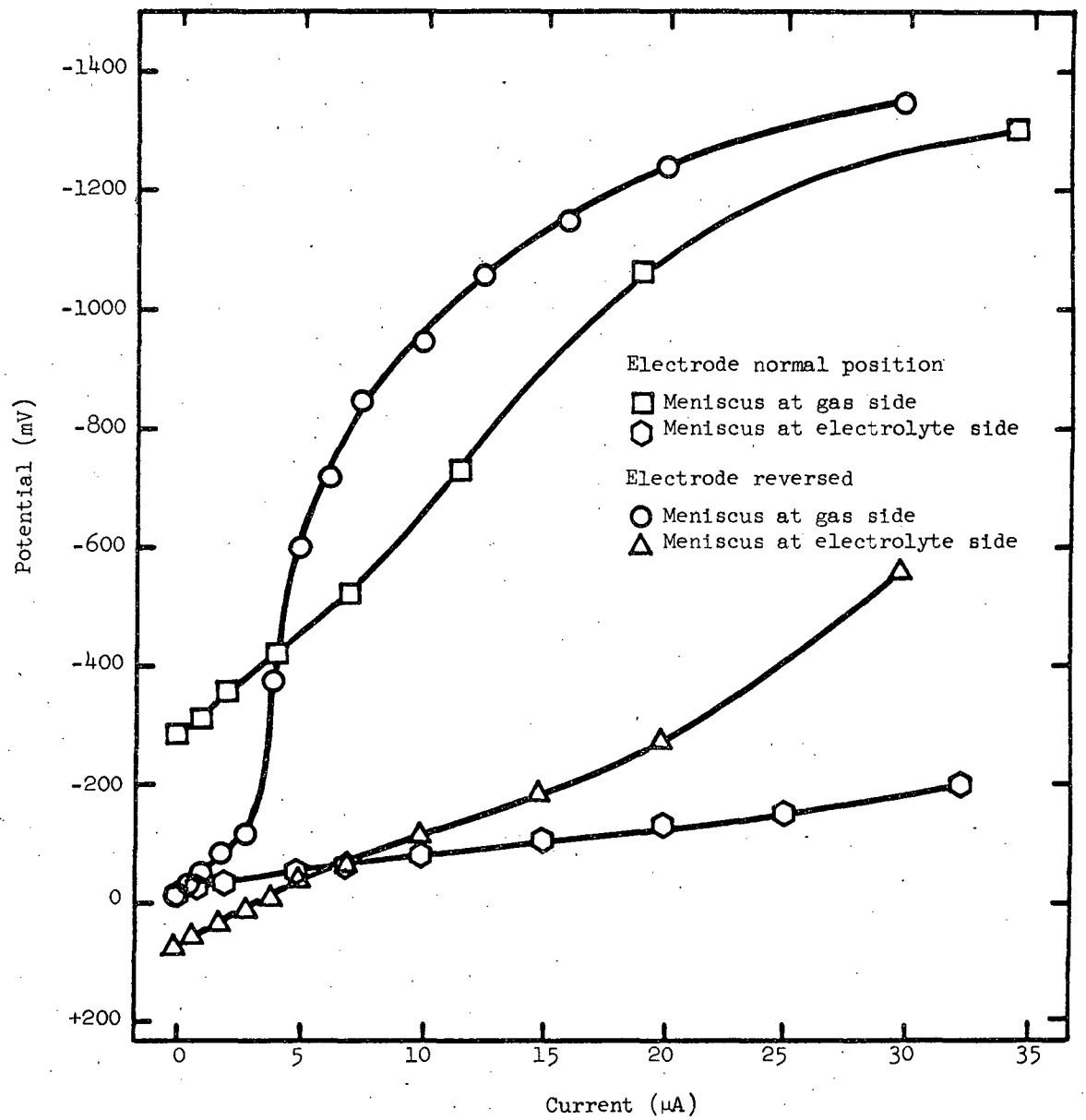

XBL 678-4383

Fig. 23 Cathode potential/current characteristics with meniscus at gas and electrolyte ends of the electrode for both normal and reversed electrode configurations.

at its two ends, differences that severe cleaning and etching procedures were not able to eliminate.* These local variations in oxygen reduction performance have precluded revision of the electrodes, using available capillary tubes, to approach desired design conditions closely enough to obtain quantitatively significant results. It appears that capillaries with more uniform inner surface must be obtained.

D. Summary

The results obtained in measurements of effects of meniscus displacements in the capillary oxygen electrode cannot be interpreted quantitatively because of the deviations in cathode operating conditions from design conditions. In fact, there was a spurious electrolyte path offering a lower resistance to the transfer of ionic species during the experimental series reported in this chapter. Moreover, it was also found that the meniscus was located at the gas end of the capillary tube. These deviations from design conditions led to certain anomalies in measurements and signals obtained, and also to the requirement of excessively high currents. The existence of the electrolyte short circuit path was later suppressed and determination of the cathode overpotential characteristics for both ends of the electrode were made, which showed differences in inner surface conditions of the capillary tube.

Nevertheless, qualitative effects of the movement of the gas-electrolyte interface were observed and a periodic response of the cathode potential relative to the reference electrode was recorded. The cathode overpotential was found to decrease as the meniscus was moved toward the gas

* The etching of the ends of the capillary tube was conducted with a current density of .2A/cm^2 for 5-20 sec in a solution of potassium ferrocyanide and sodium cyanide (60 g of each per liter of solution).

end side of the capillary tube, and to increase as the meniscus was moved toward the electrolyte side. The amplitude of this response, which was not in phase with the piston movement, was found to decrease with increasing frequencies and to increase with increasing piston displacements.

VI. CONCLUSIONS

The effects of periodic displacements of the gas-electrolyte interface in a porous gas electrode were not measured quantitatively in this study, as intended, because of extensive deviations of the conditions in the electrode from experimental design conditions. However, qualitative effects of the meniscus movement were observed and a periodic response of the cathode potential (vs the mercury/mercuric oxide reference electrode) was recorded. It shows a decrease in overpotential during the advance of the meniscus toward the gas filled part of the capillary and an increase during displacement in the opposite direction.

These results are in agreement with what could be expected on the basis of a film electrode model, and indicate the desirability of conducting further experiments using a capillary tube of uniform surface properties mounted in the manner developed for the final measurements of this work. Also, additional provisions must be made to allow location of the meniscus at a position in the capillary tube well removed from either end. With these improvements, measurements of the type described here should serve to provide valuable information on the behavior of mass transport processes in film type gas electrodes.

ACKNOWLEDGEMENTS

I wish to express my appreciation to Prof. E. A. Grens II for his direction and encouragement during the course of this work, and am indebted to Prof. R. J. Ayen and Prof. I. Fatt for their review of the thesis.

The helpful discussions with Prof. J.S. Newman and other members of the electrochemistry group are gratefully acknowledged.

This work was performed under the auspices of the United States Atomic Energy Commission.

REFERENCES

1. W. R. Grove, Phil. Mag., 14, 127 (1839).

2. W. R. Grove, Phil. Mag., 21, 417 (1842).

3. C. Wagner, Polarization Characteristics of Gas Electrodes in Stagnant Electrolytes, Unpublished paper dated June 13, 1957.

4. E. Justi, K. Bischoff and H. Spengler, Akad. der Wissenschaften und der Literature, No. 1, 3-26 (1956).

5. E. Justi and A. Winsel, Kalte Verbrennung - Fuel Cells, (Franz Steiner, Verlag, Wiesbaden, 1962), Chapter 3.

6. F. G. Will, J. Electrochem. Soc. 110, 145-151 (1963).

7. F. G. Will, J. Electrochem. Soc., 110, 151-160 (1963).

8. R. P. Iczkowski, J. Electrochem. Soc. 111, 1078-1086 (1966).

9. E. A. Grens II, R. M. Turner, and T. Katan, Adv. Energy Conversion, 4, 109-119 (1964).

10. T. Katan, S. Szpak and E. A. Grens II, J. Electrochem. Soc., 112, 1166-1171 (1965).

11. J. A. Rockett and R. Brown, J. Electrochem. Soc., 113, 207-213 (1966).

12. D. N. Bennion, Phenomena at a Gas-Electrode-Electrolytic Interface, Ph.D. Thesis, University of California, Department of Chemical Engineering, Berkeley, 1964.

13. A. G. Pshenichnikov, G. E. Shnaider, and R. Kh. Burshtein, Sov. Electrochem., 1, 363 (1965).

14. R. H. Muller, Paper presented at the Toronto Meeting of the Electrochem. Society, May 1964.

15. R. H. Muller, Paper presented at the Washington meeting of the Electrochem. Society, October 1966.

16. E. N. Lightfoot and V. Ludviksson, J. Electrochem. Soc., 113, 1325-1329 (1966).

17. E. N. Lightfoot, J. Electrochem. Soc., 113, 614-619 (1966).

18. Union Carbide Corporation, Study Program to Improve Fuel Cell Performance by Pulsing Techniques, NASA Contract NAS 3-2752 (1964) by M. L. Kronenberg and K. V. Kordesch.

19. B. E. Conway, Electrochemical Data, Elsevier Publishing Company, New York, 1952), p. 348.

20. R. E. Davis, G. L. Horvath, and C. W. Tobias, The Solubility and Diffusion Coefficient of Oxygen in KOH, Department of Chemical Engineering, University of California, Berkeley, California.

21. T. Katan and S. Szpak, Bureau of Naval Weapons Contract, NW-64-0597-f., June 1965.

22. S. Z. Beer and Y. L. Sandler, J. Electrochem. Soc. 112, 1133-1136 (1965).

23. P. Pascal, Nouveau traité de Chimie Minérale, (Masson-Tome XVII, 1956) p. 739.

24. D. Ives and G. Janz, Reference Electrodes, (Academic Press, New York, 1961), p. 335.

25. G. Charlot and D. Bezier, Analyse quantitative Minerale, (Masson, 1965) p. 38.

26. J. O'M. Bockris, Modern Aspects of Electrochemistry, (Academic Press, New York, 1954), p. 260.

27. A. Azzam, J. O'M. Bockris, B. E. Conway and H. Rosenberg, Trans. Faraday Soc., 46, 918 (1950).

28. E. Yeager, The Measurement of Polarization, Western Reserve University, Cleveland, Ohio.

29. P. Pascal, Nouveau traité de Chemie Minérale (Masson-Tome XIV, 1956) p. 783.

30. M. Bonnemay, G. Bronoel and E. Levart, Electrochem. Acta., 9, 727-739 (1964).

31. W. M. Latimer, The Oxidation States of the Elements and Their Potentials in Aqueous Solutions, (Prentice-Hall, Inc., New York , 1952) p. 38 and 198.

32. Landolt-Bornstein, Zahlenwerte und Funktionen aus Physik-Chemic-Astronomic-Geophysik-Technik., II Band - 7 Teil, Electrische Eigenschaften II, Table 2 763, p. 54.

APPENDIX A

Reaction at the Counter Electrode

Two principal electrochemical reactions may take place on a nickel anode in potassium hydroxide. Since one of these reactions would evolve oxygen, it is important to determine that it does not occur. The two reactions considered are:

$$Ni + 2OH^- \rightarrow Ni(OH)_2 + 2e^- \qquad (1)$$

$$4OH^- \rightarrow O_2 + 2H_2O + 4e^- \qquad (2)$$

By consideration of the change of free energy of both reactions, it can be shown that the normal equilibrium potentials of the two systems are respectively

$$+ .717 \text{ volt} \quad \text{and} \quad - .400 \text{ volt}$$ [31]

Nernst's equation applied to the Eq. (1) yields:

$$E_1 = .717 - \frac{RT}{2F} \text{ Log } \frac{a_{Ni(OH)_2}}{a_{Ni} \cdot (a_{OH^-})^2}$$

With the assumption, as a first approximation of unit activity coefficient of the hydroxyl ions and unit activity for nickel hydroxide, the above expression reduces to:

$$E_1 = .717 - \frac{RT}{2F} \text{ Log } \frac{1}{[OH^-]^2}$$

$$E_1 = .717 + 0.0591 \log [OH^-]$$

Nernst's equation applied to the second reaction yields:

$$E_2 = -.400 - \frac{RT}{4F} \text{ Log } \frac{a_{O_2} \cdot \left(a_{H_2O}\right)^3}{\left(a_{OH^-}\right)^4}$$

For ideal behavior of the gas, it reduces to:

$$E_2 = -.400 - \frac{0.0591}{4} \log \frac{P_{O_2}}{[OH^-]^4}$$

The reaction (2) would take place if E_2 were greater than E_1. For $[OH^-] = 2$, this would imply:

$$-.400 - \frac{0.0591}{4} \log \frac{P_{O_2}}{(2)^4} > .717 + 0.0591 \log 2$$

or

$$P_{O_2} < 2.6 \times 10^{-76} \text{ atm}$$

This oxygen pressure would correspond to an extremely small concentration of dissolved gas in the electrolyte, much smaller than the concentration of most impurities. Therefore, Eq. (2) should not take place at a significant rate and the hydroxyl ions will react at the counter electrode to form nickel hydroxide.

APPENDIX B

Estimation of Mass Transport Time Constants

The mass transport time constant for the electrochemical system investigated may be estimated either for the diffusion of oxygen through the electrolyte film, for the re-establishment of a gradient of ionic species in the film along the pore wall, or for the consumption by reaction of dissolved oxygen molecules overrun by the meniscus during its movement.

The time constant for diffusion of gas through a liquid is proportional to the square of the liquid thickness and inversely proportional to the gas diffusion coefficient. Therefore, assuming the film thickness to range between .1μ and 1μ, the time constant to re-establish the gas concentration on the electrode surface can be expected to be:

$$\tau_1 = \frac{\left(10^{-5} \text{ to } 10^{-4}\right)^2}{10^{-5}} = 10^{-5} \text{ to } 10^{-3} \text{ sec}$$

The time constant for re-establishment of the gradient of ionic species along the pore wall after any mixing of the film is also proportional to the square of the liquid length and inversely proportional to the diffusion coefficient of the ions considered. Under the assumption that the reaction takes place over a length equal to between hundreds and thousands film thicknesses, this time constant is:

$$\tau_2 = \frac{\left(10^{-3} \text{ to } 10^{-1}\right)^2}{4.10^{-5}} = 2.5 \times 10^{-2} \text{ to } 2.5 \times 10^{2} \text{ sec.}$$

Finally, the time constant for the gas dissolved in the electrolyte film in the absence of meniscus movement to react at the electrode surface behind the meniscus after its displacement toward the gas filled part of the capillary tube is given very approximately by the following expression:

$$\tau_3 = \frac{\pi \cdot F \cdot C_g^o \cdot l \cdot e \cdot d}{i}$$

Where: C_g^o = dissolved gas concentration

l = amplitude of the meniscus displacement

e = film thickness

d = pore diameter

i = current

For: $C_g^o = 4 \times 10^{-7}$ g mole/cm^3

$l = .3$cm

$d = 1.5 \times 10^{-2}$ cm

$i = 10^{-5}$ A.

This yields

$$\tau_3 \simeq 6 \times 10^{-3} \text{ sec.}$$

Therefore, the mass transport time constant for the electrode may be of the order of a small fraction of a second up to many seconds. However, since it is doubtful that the gradient of ionic species is re-established between two displacements of the gas-electrolyte interface in these experiments, frequencies ranging from .05 to 1000 Hz may be investigated.

APPENDIX C

Determination of the Current Range to be Investigated

According to the analysis derived by Grens[9] for a model of film porous gas electrode, the superficial current density in the cylindrical pore with a reaction given by

$$G + ne \rightarrow \mu H_2O + v S_i^{z_i}$$

can be expressed in terms of a dimensionless current density in the film, I^o

$$j = - \frac{2p F z_i D_i C_i^o}{r} I^o \quad A/cm^2$$

Where:

j	=	current density
p	=	electrode porosity
F	=	Faraday's constant
z_i	=	charge number of species i
D_i	=	diffusion coefficient of species i
C_i^o	=	reference concentration of species i
r	=	pore radius

I^o is developed as a function of electrode potential for the oxygen electrode in the cited reference.

Applied to the case of the present capillary tube electrode, the above expression can be transformed to give the total current passing through the electrode:

$$I = -2 \pi r F z_1 D_1 C_1^o I^o \text{ A.}$$

For the system considered in these experiments, the following values are utilized:

$$z_1 = -1$$

$$C_1^o = 5 \times 10^{-3} \text{ g mole/cm}^3$$

$$D_1 = 4 \times 10^{-5} \text{ cm}^2\text{/sec}$$

$$r = 75 \times 10^{-4} \text{ cm}$$

$$F = 96{,}500 \text{ C/equiv.}$$

This yields:

$$I \approx 10^{-3} I^o$$

Since the value of I^o ranges from about 5×10^{-5} at 2mV overpotential to about 5×10^{-3} at 100 mV overpotential, the currents to be investigated should range between 5×10^{-8} A and 5×10^{-6} A.

APPENDIX D

Piston Displacement Amplitudes

The mechanical drive system described in Chapter 3 provides various piston displacement amplitudes. If O, P, and W represent respectively the axis of the level pin, the piston carrier, and the level wheel, the ratio piston displacement/cam eccentricity is equal to 2 OP/OW. The amplitudes that can be obtained with the two eccentric cams for the eight possible positions of the lever pin are given in the following table.

Table 4

Piston Displacement Amplitudes

	OP_{mm}	30	43	55	67.2	80	98	110.8	120
Cam 1 ecc=.66mm	piston displacement mm	.26	.41	.58	.78	1.06	1.58	2.11	2.64
Cam 2 ecc=.2mm	piston displacement mm	.08	.13	.18	.24	.32	.48	.64	.80

APPENDIX E

Resistance of Electrolyte Within the Capillary Tube Electrode

Since the reaction takes place essentially under the electrolyte film above the meniscus, the ohmic voltage drop inside the capillary tube is proportional to the current and to the resistance of the electrolyte filled part of the electrode. The maximum ohmic drop occurs for the meniscus located at the gas end of the capillary tube. The equivalent conductance of a 2N solution of potassium hydromide is 180 Ω^{-1} cm^2/mole.[32] Since the resistivity ρ is given by the relation $\rho = \frac{1000}{C\Lambda}$ (where C is the electrolyte concentration in mole/liter), it is equal to 2.8 Ω cm. This yields a resistance of the flooded capillary tube of:

$$R = \rho \frac{\ell}{\pi d^2/4}$$

where ℓ = tube length

d = tube diameter

For ℓ = 2. cm and d = 15×10^{-3} cm

$$R \simeq 32 \text{ K } \Omega$$

This high resistance of the electrolyte within the capillary tube should give an ohmic voltage drop of 1.3 volt for a current of 40μA when the meniscus is located at the gas end of the electrode.

APPENDIX F

Oscillographic Recorder Traces for Experimental Runs

Characteristic records of the phenomena observed at various frequencies, piston amplitudes, and currents are shown in the following pages. Traces on each figure are respectively from the left to the right for the piston position, the cathode potential variation and the current. For the potential and current records, zero suppression has been used to shift the mean value approximately to the center of the record band. The amplitude of the piston movement, the mean value of the cathode potential relative to the mercury-mercuric oxide reference electrode, and the mean value of the current are indicated under each record, together with appropriate scale calibrations given as sensitivities in units per chart line. Timing marks at one second intervals are also shown. The left side of the trace recorded for the piston displacement corresponds to the lowest position of the plunger into the electrolyte compartment and thus to the meniscus location nearest the gas side of the capillary tube. For the cathode potential curve, increasing overpotentials are represented by trace displacement to the right.

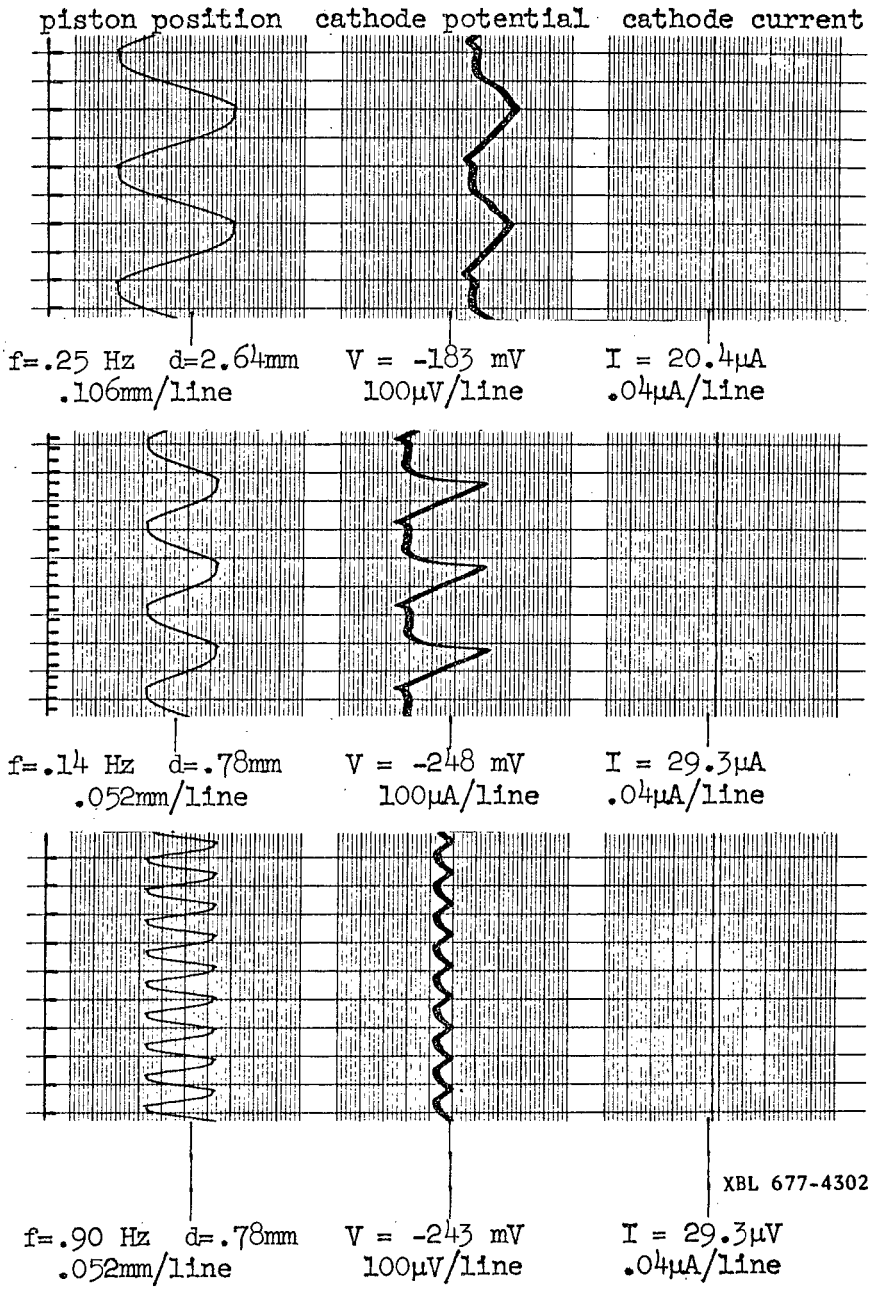

Fig. F1 Oscillographic records for Experimental Series No. 1.

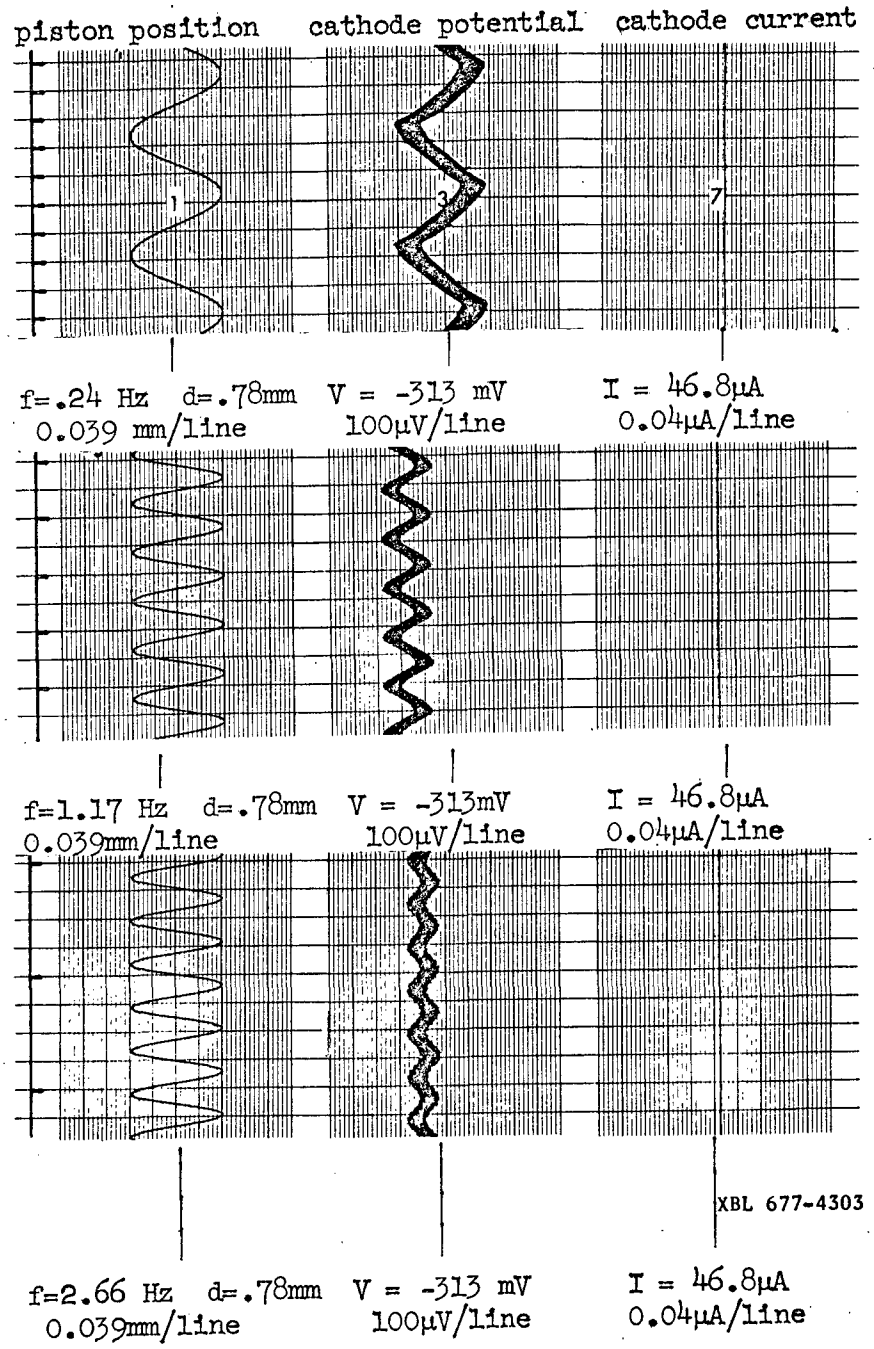

Fig. F2 Oscillographic record for a current of 46.8μA and piston displacement of .78mm.

Experimental Series No. 4.

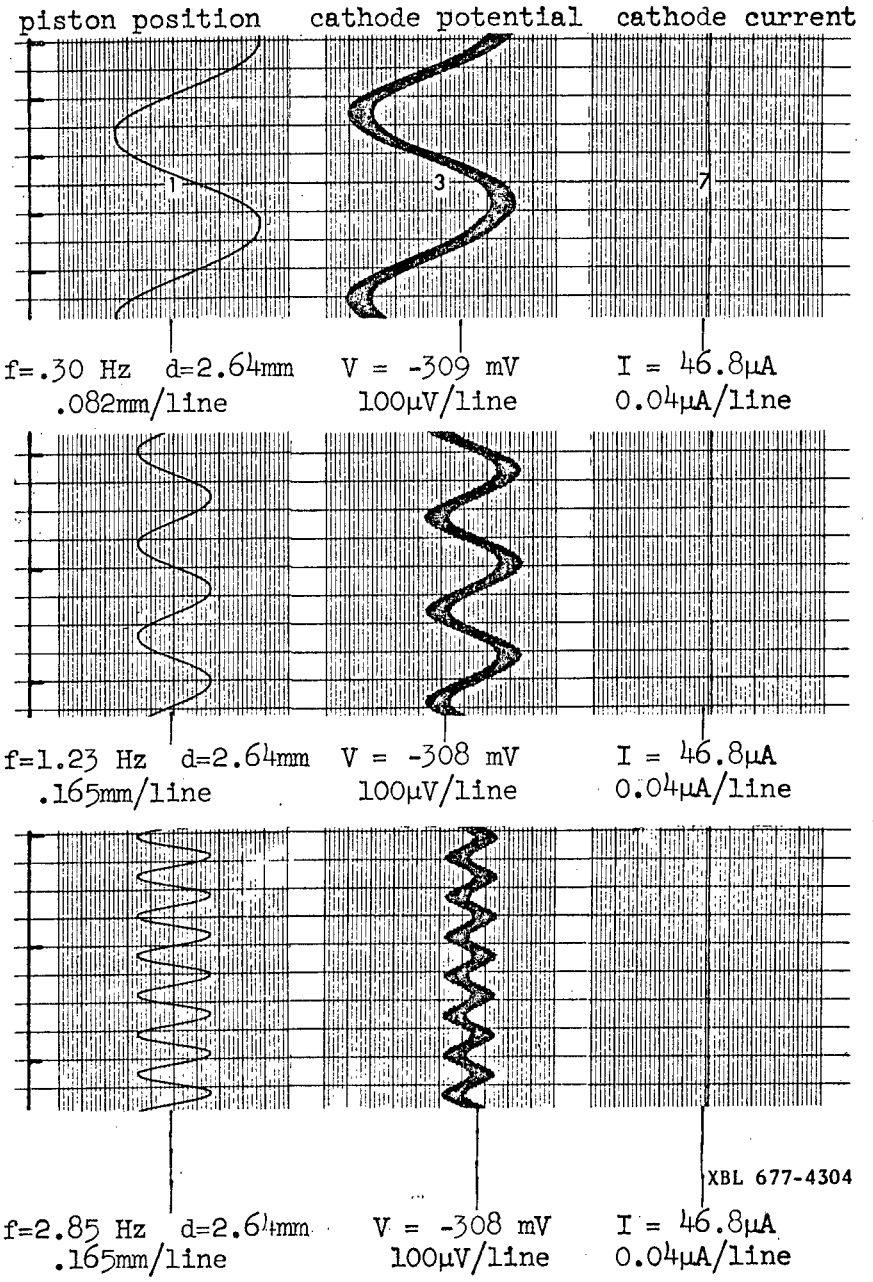

Fig. F3 Oscillographic records for a current of 46.8μA and piston displacement of 2.64mm.

Experimental Series No. 4.

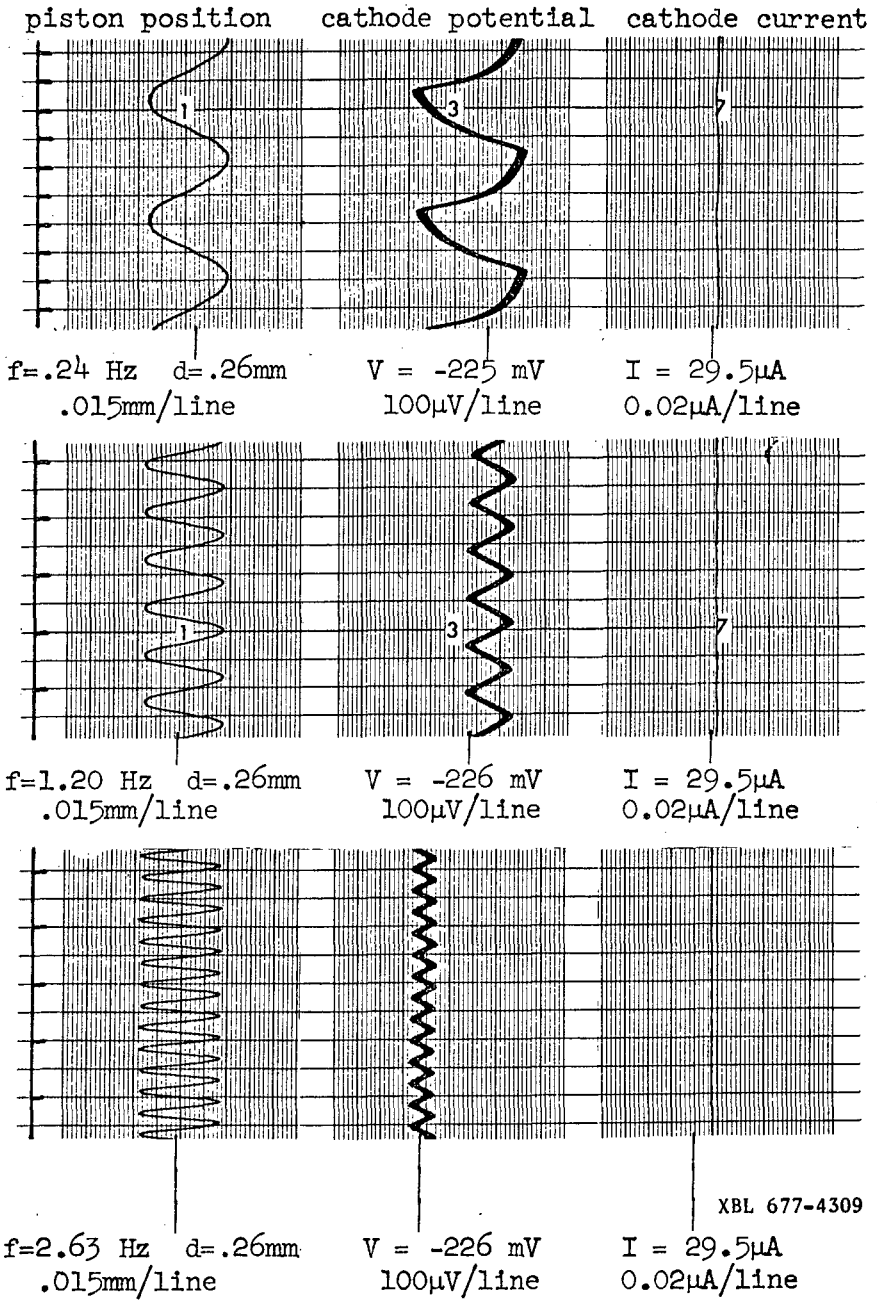

Fig. F4 Oscillographic records for a current of 29.5μA and piston displacement of .26mm.

Experimental Series No. 3.

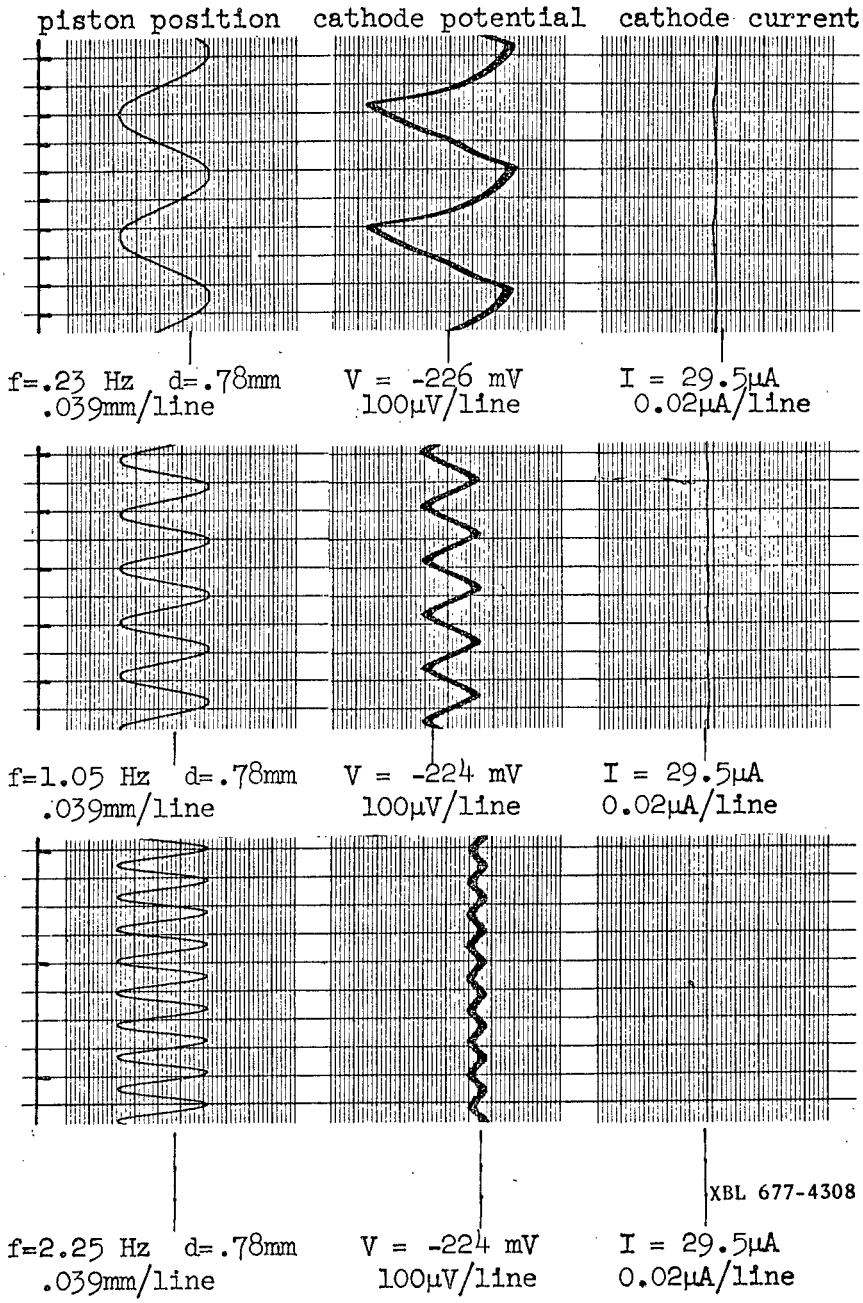

Fig. F5 Oscillographic records for a current of 29.5μA and piston displacement of .78mm.

Experimental Series No. 3.

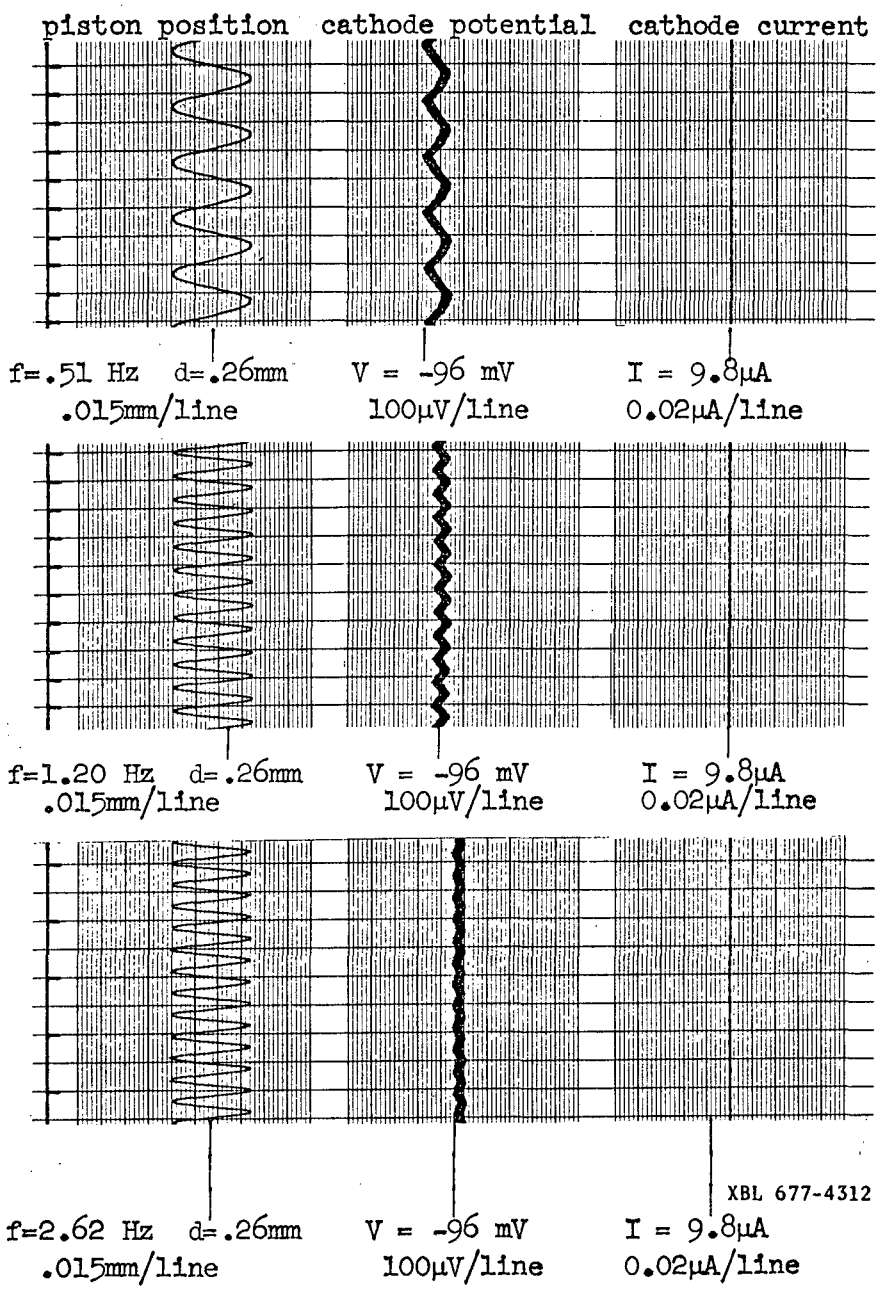

Fig. F6 Oscillographic records for a current of 9.8μA and piston displacement of .26mm.

Experimental Series No. 3.

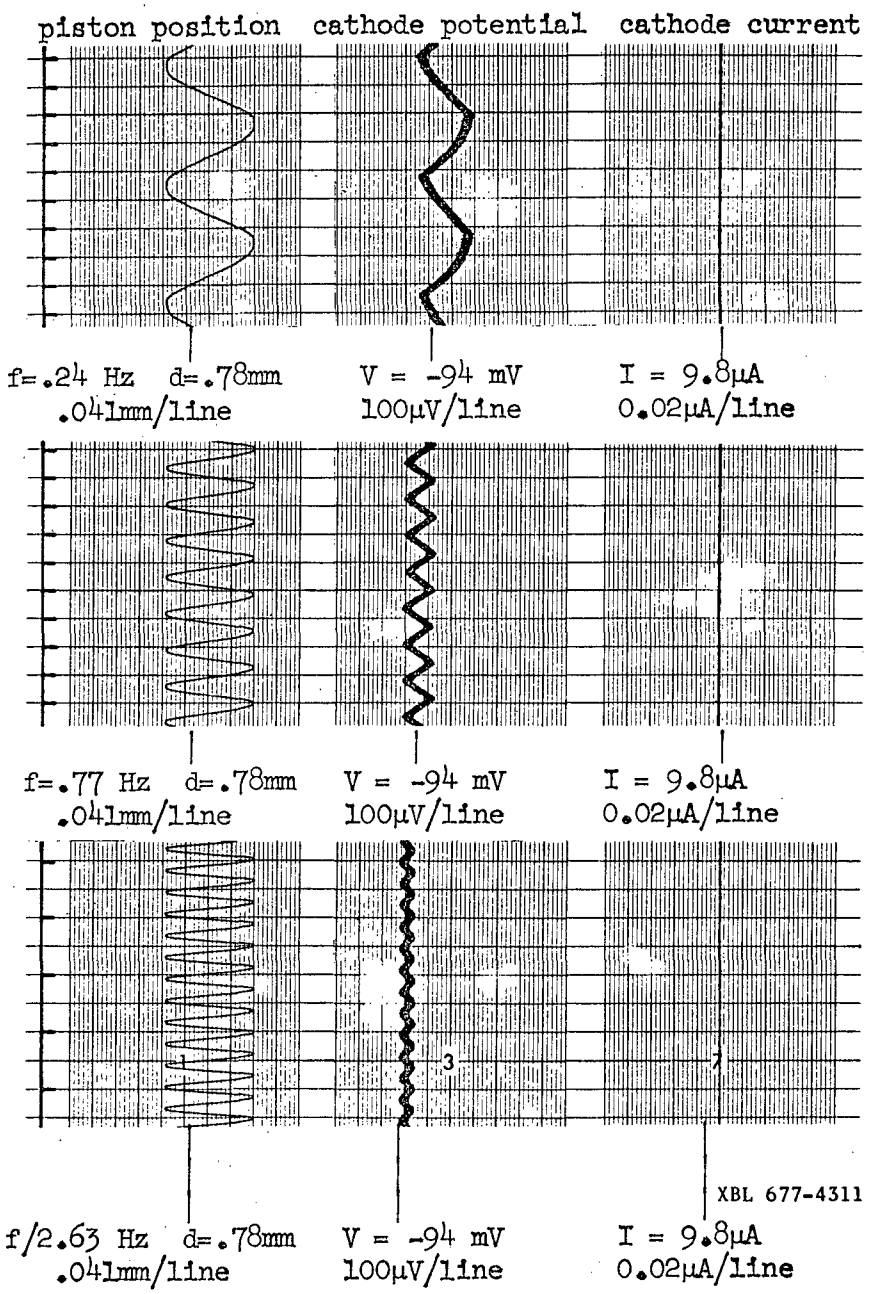

Fig. F7 Oscillographic records for a current of 9.8μA and piston displacement of .78mm.

Experimental Series No. 3.

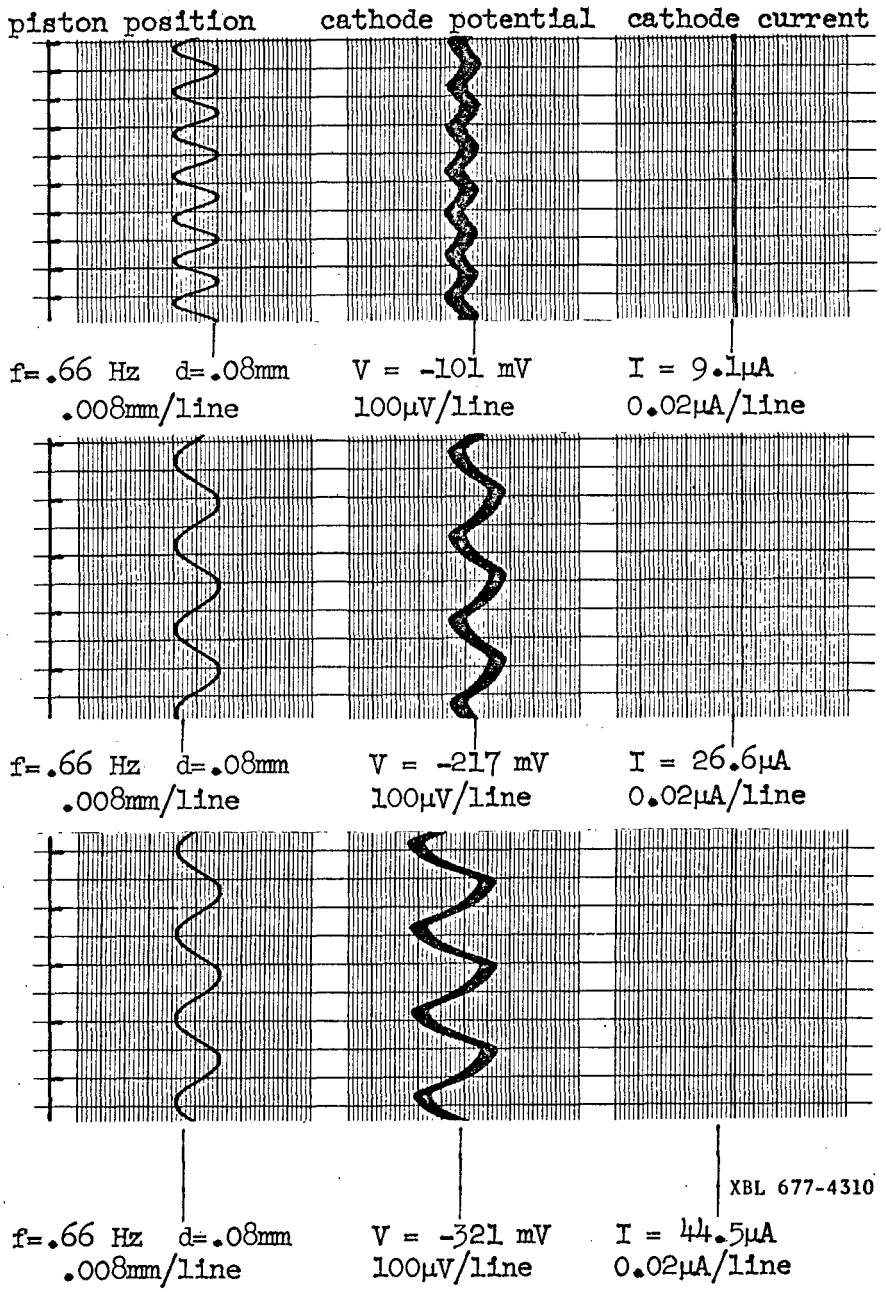

Fig. F8 Oscillographic records for a frequency of .66 Hz and piston displacement of .08mm.

Experimental Series No. 4.

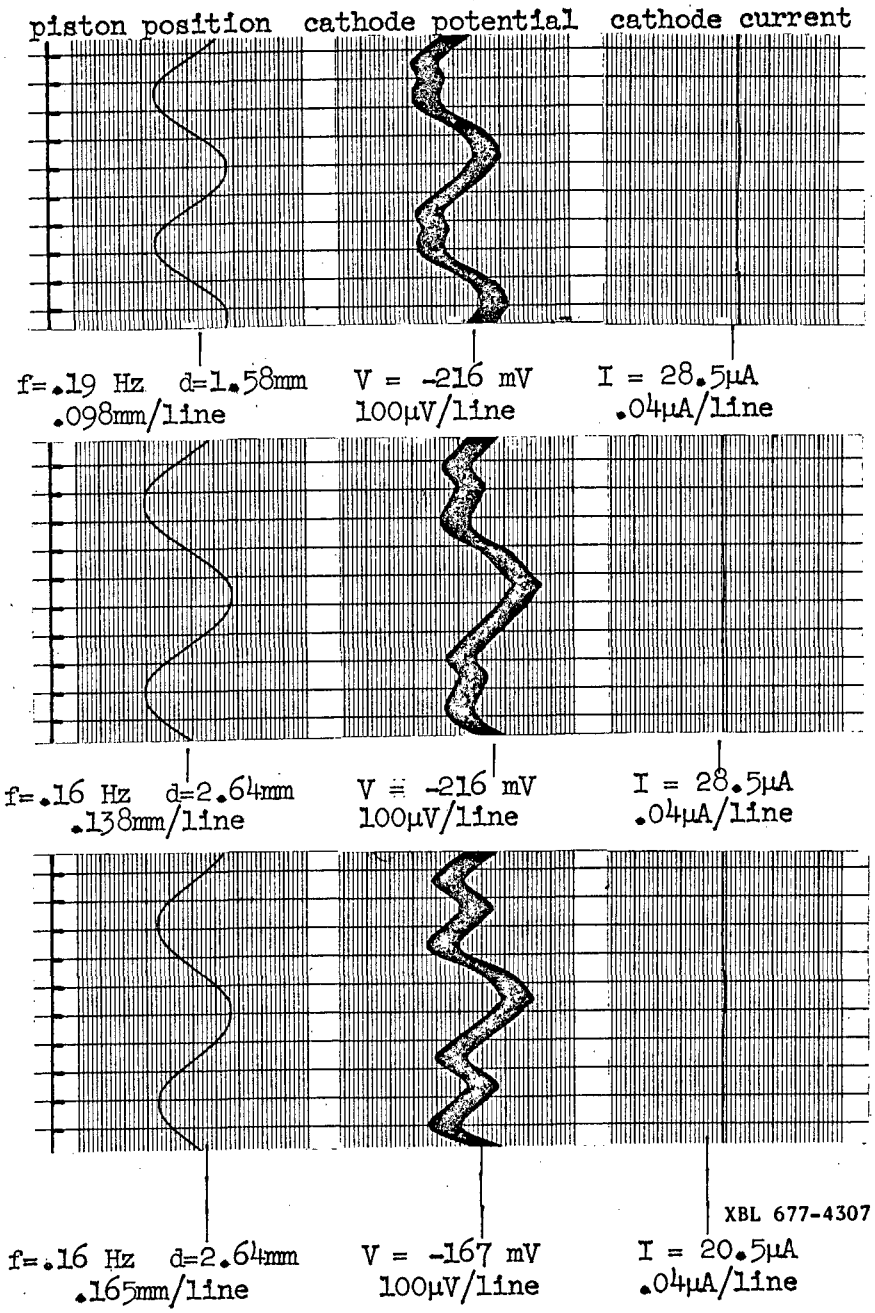

Fig. F9 Oscillographic records for Experimental Series No. 4.

This report was prepared as an account of Government sponsored work. Neither the United States, nor the Commission, nor any person acting on behalf of the Commission:

A. Makes any warranty or representation, expressed or implied, with respect to the accuracy, completeness, or usefulness of the information contained in this report, or that the use of any information, apparatus, method, or process disclosed in this report may not infringe privately owned rights; or

B. Assumes any liabilities with respect to the use of, or for damages resulting from the use of any information, apparatus, method, or process disclosed in this report.

As used in the above, "person acting on behalf of the Commission" includes any employee or contractor of the Commission, or employee of such contractor, to the extent that such employee or contractor of the Commission, or employee of such contractor prepares, disseminates, or provides access to, any information pursuant to his employment or contract with the Commission, or his employment with such contractor.

LRL